NEAR INFRARED FLUORESCENCE MOLECULAR IMAGING FOR CANCER DIAGNOSTICS

Dimitrios Gorpas
Electrical and Computer Engineer, PhD

Information Technologies Institute, CERTH 2012

Introduction

Among the most important problems in medical imaging is the three-dimensional reconstruction of biostructures embedded into tissues.

- Need for non-invasive and safe for the patients techniques,
- Need for reconstruction accuracy and time efficacy.

Fluorescence imaging is advancing to a very essential tool for medical imaging and diagnosis, mainly for cancer diagnosis.

- Progress in fluorescent probes technology and optical imaging modalities.
- Data quantification and processing is now more realistic and possible.

Outline

- The fluorescence phenomenon.
- Fluorescence molecular imaging - the problems.
- Image acquisition systems.
- Light propagation models.
- Conclusion.

Luminescence

Light emission from a medium, which is not due to high temperature, is called luminescence.

Since luminescence is actually energy leaving the medium, some kind of energy absorption should precede light emission...

...and thus we have:

- Electroluminescence (LEDs),
  Substance excitation due to electric current.

- Radioluminescence (emergency exit signs),
  Substance excitation due to ionizing radiation.

- Chemiluminescence (glow sticks) and
  Substance excitation due to chemical reaction.
- Photoluminescence (safety signs).
  Substance excitation due to photon absorption.

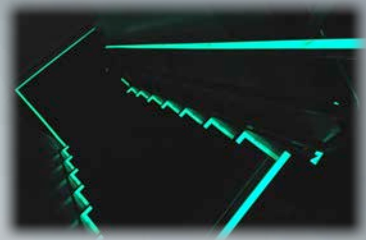

Luminescence

Light emission from a medium, which is not due to high temperature, is called luminescence.

Since luminescence is actually energy leaving the medium, some kind of energy absorption should precede light emission…

…and thus we have:

- Electroluminescence (LEDs),
  Substance excitation due to electric current.
- Radioluminescence (emergency exit signs),
  Substance excitation due to ionizing radiation.
- Chemiluminescence (glow sticks) and
  Substance excitation due to chemical reaction.
- Photoluminescence (safety signs).
  Substance excitation due to photon absorption

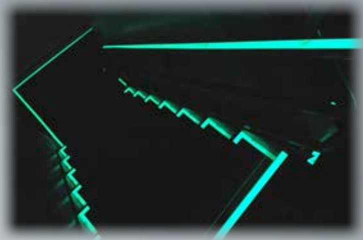

Light propagation in random media

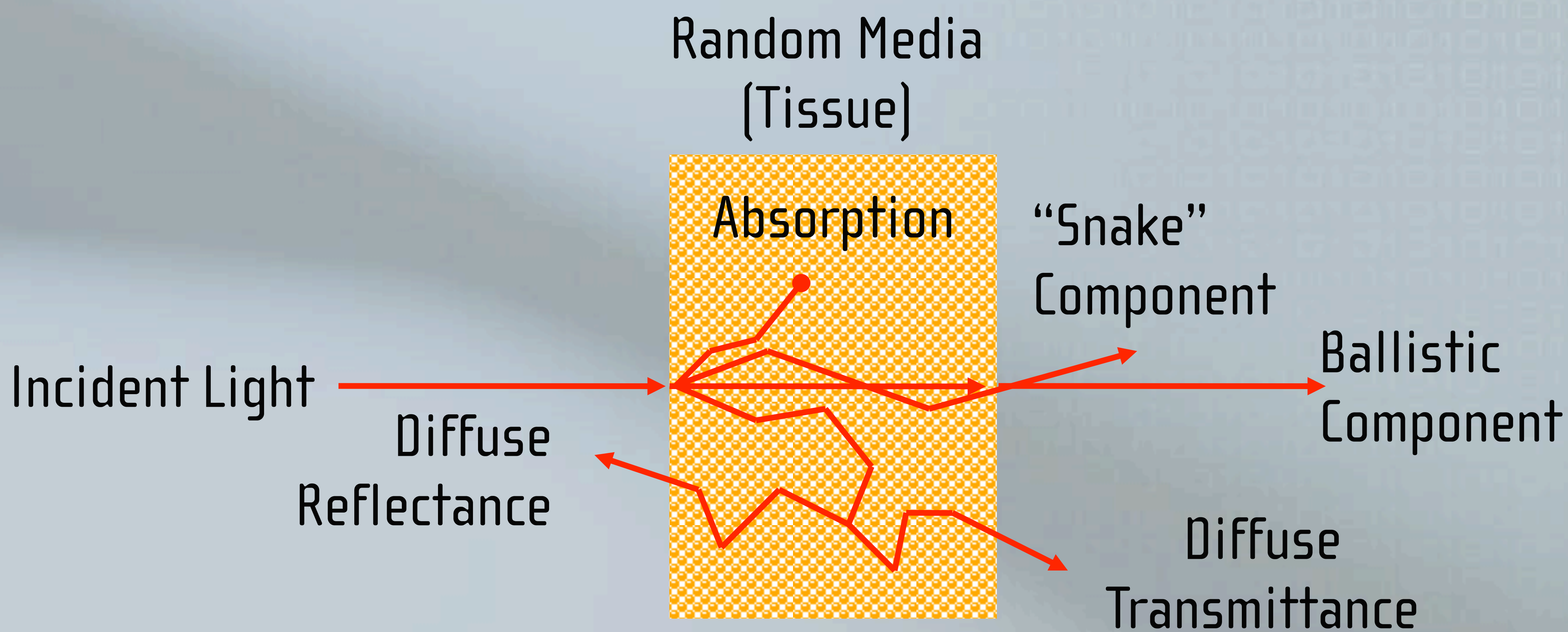

Light propagation in random media *(cont.)*

- **Absorption coefficient**: The inverse quantity corresponds to the mean depth a photon travels inside the medium before it is absorbed.

  Beer's Law: $$I(x) = I_0 \cdot e^{-\mu_a \cdot x}$$

- **Scattering coefficient**: The inverse quantity corresponds to the mean depth a photon travels inside the medium before it is scattered.

  Equivalent to Beer's Law: $$I(x) = I_0 \cdot e^{-\mu_s \cdot x}$$

- **Penetration depth**: The depth of the medium where light intensity equals to 37% (1/e) of the incident light intensity. This quantity equals to the inverse of the attenuation coefficient $\mu_t = \mu_a + \mu_s$.

  Lambert Law: $$I(x) = I_0 \cdot e^{-\mu_t \cdot x}$$

Jablonski Diagram

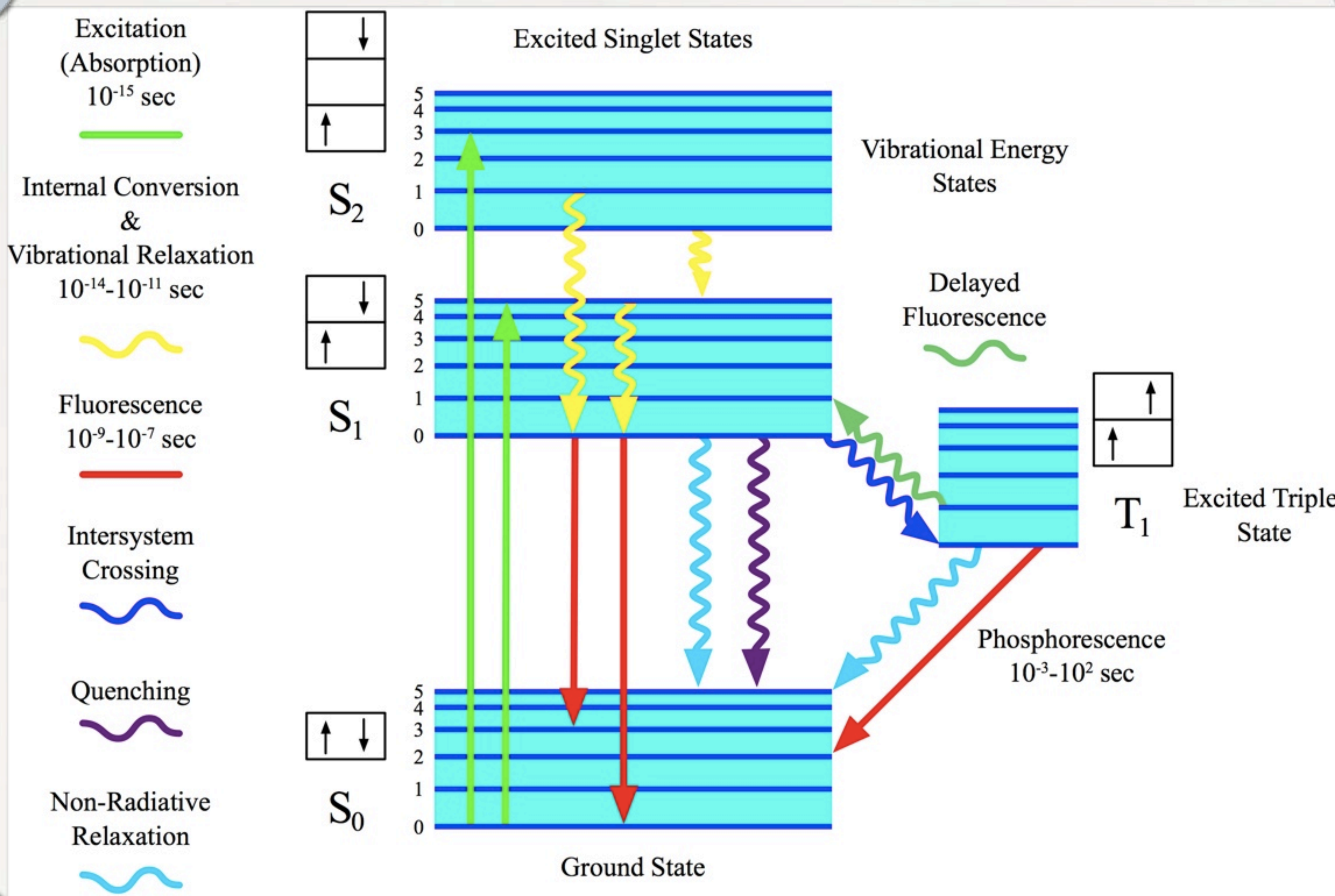

Stokes Shift

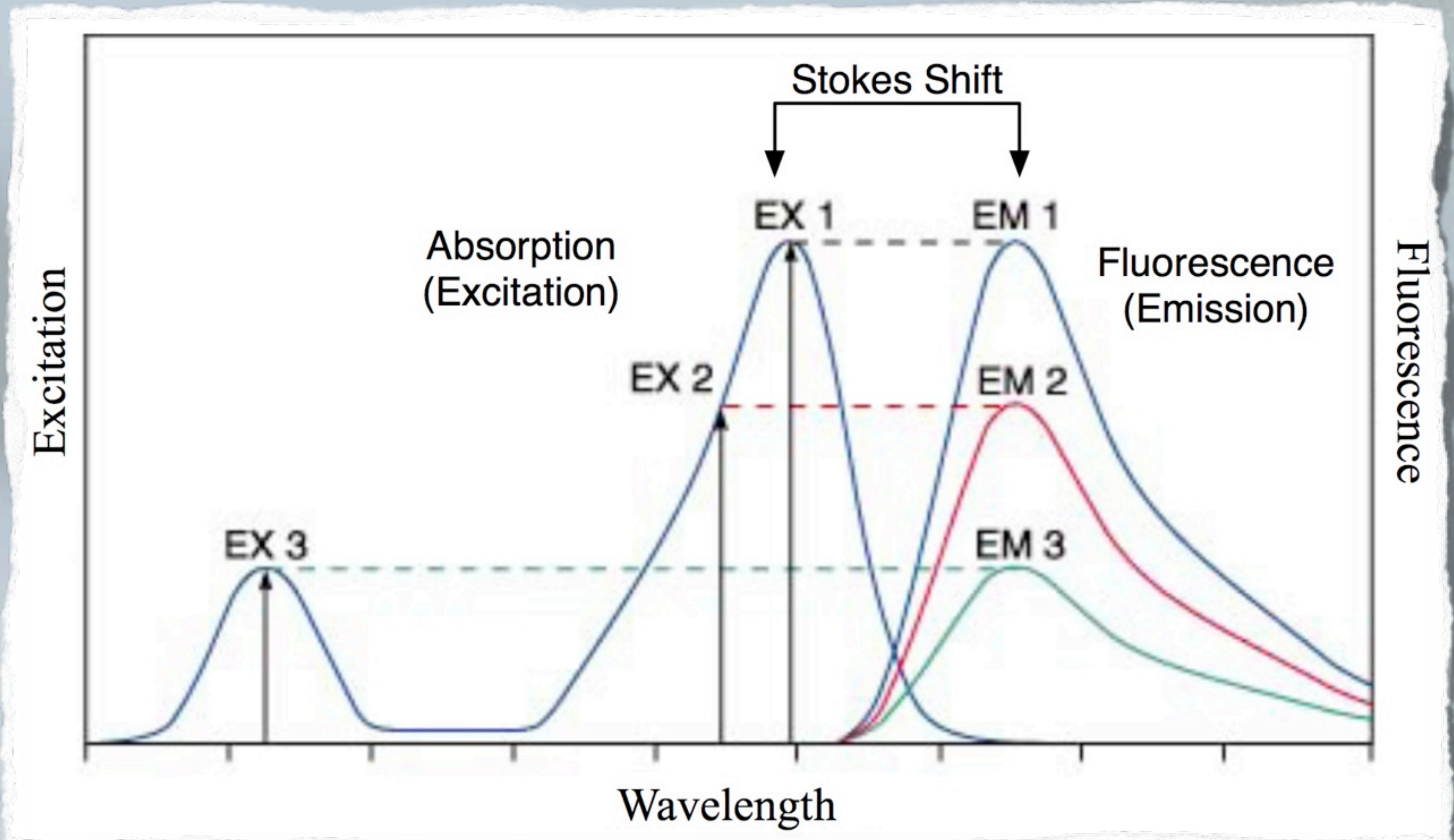

$$\lambda = \frac{h \cdot c}{E}$$

h = Planck constant = $6.626 \cdot 10^{-34}$ J $\cdot$ s

c = speed of light = $3 \cdot 10^{8}$ m $\cdot$ sec^{-1}

Have I ever "Seen" Fluorescence??

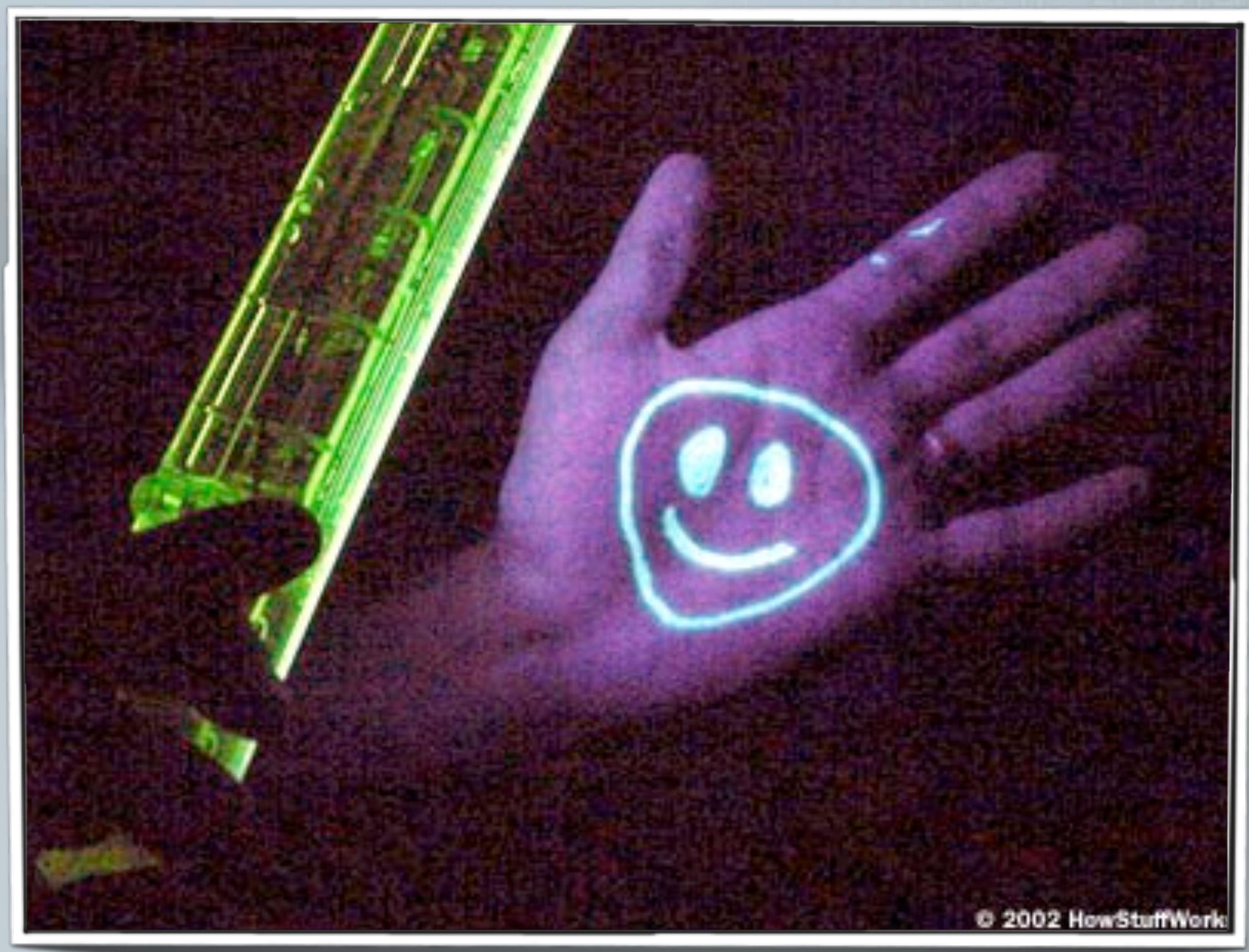

Have I ever "Seen" Fluorescence??

Have I ever "Seen" Fluorescence??

Have I ever "Seen" Fluorescence??

Autofluorescence of Our Body

- **Autofluorescence:** Emission of fluorescence without the need for exogenous fluorophores.

Chromophore	λ_{exc} (nm)	λ_{em} (nm)
Tryptophan	275	350
Collagen	340 270 285	395 395 310
Elastin	460 360 425 260	520 410 490 410
NADH	350	460
Endogenous Porphyrins	400	610, 675

Absorption of Our Body

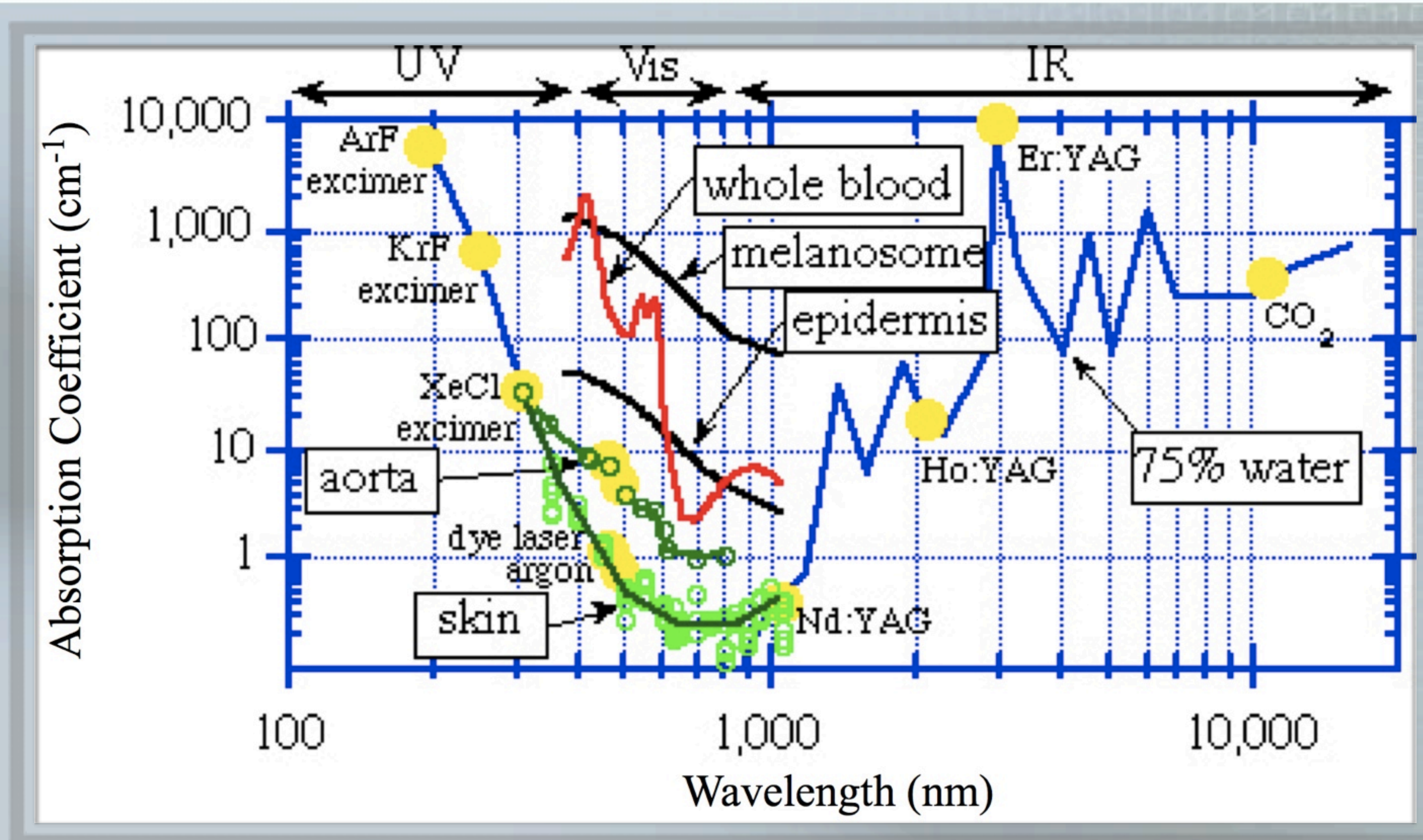

- **Absorption dominated spectral range:** $\lambda<250$ nm and $\lambda>2000$ nm.
- **Scattering dominated spectral range:** 600 nm $< \lambda <$ 1200 nm. *Optical window*.
- **Comparable scattering and absorption:** all the other wavelengths.

So...why Near IR Wavelengths?

- Most of the tissue endogenous fluorophores absorb at the region λ<600 nm.
- The same as blood and most of all other tissue molecules.

For wavelengths below 600 nm the light presents very small penetration depth.

(Very useful in multi-view machine vision systems with structured light projection)

- Within the optical window, tissue is a scattering dominated medium and thus light can propagate a few centimeters before it is absorbed.
- Autofluorescence does not exist in the optical window and thus the acquired fluorescence is the signal of interest.

Fluorophores Technology

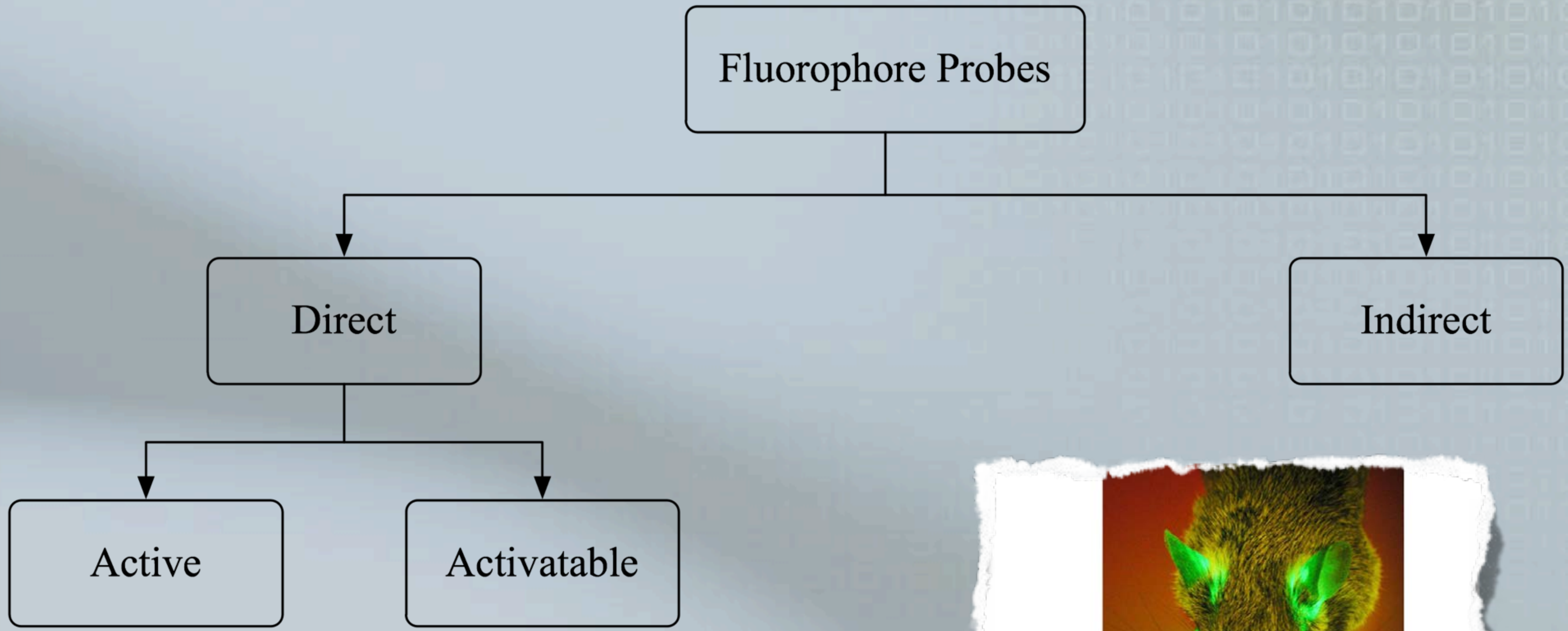

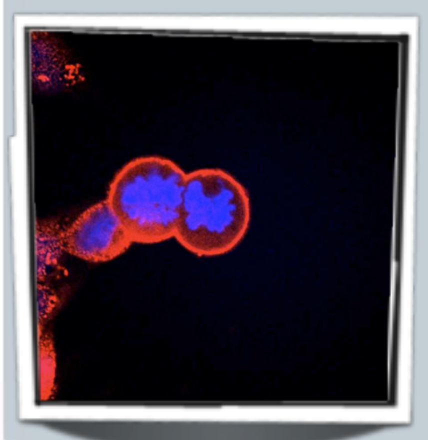

Outline

- The fluorescence phenomenon.
- Fluorescence molecular imaging - the problems.
- Image acquisition systems.
- Light propagation models.
- Conclusion.

Fluorescence Molecular Imaging

The solution of the reconstruction problem, in the context of fluorescence molecular imaging, corresponds to the estimation of the fluorophores distribution within the investigated medium, when:

- the amount of guided light and
- the measured data on the boundary of the object are given.

The fluorescence molecular imaging investigated characteristics are:

- the absorption coefficient values of the fluorophores,
- their three-dimensional distributions and
- their fluorescence lifetime.

The Forward Problem in Fluorescence Molecular Imaging

The **forward problem** in fluorescence imaging is to solve the measurable data, which are the intensity values recorded by the detector on the surface of the inspected region, when the fluorescence distribution and the input light sources are given.

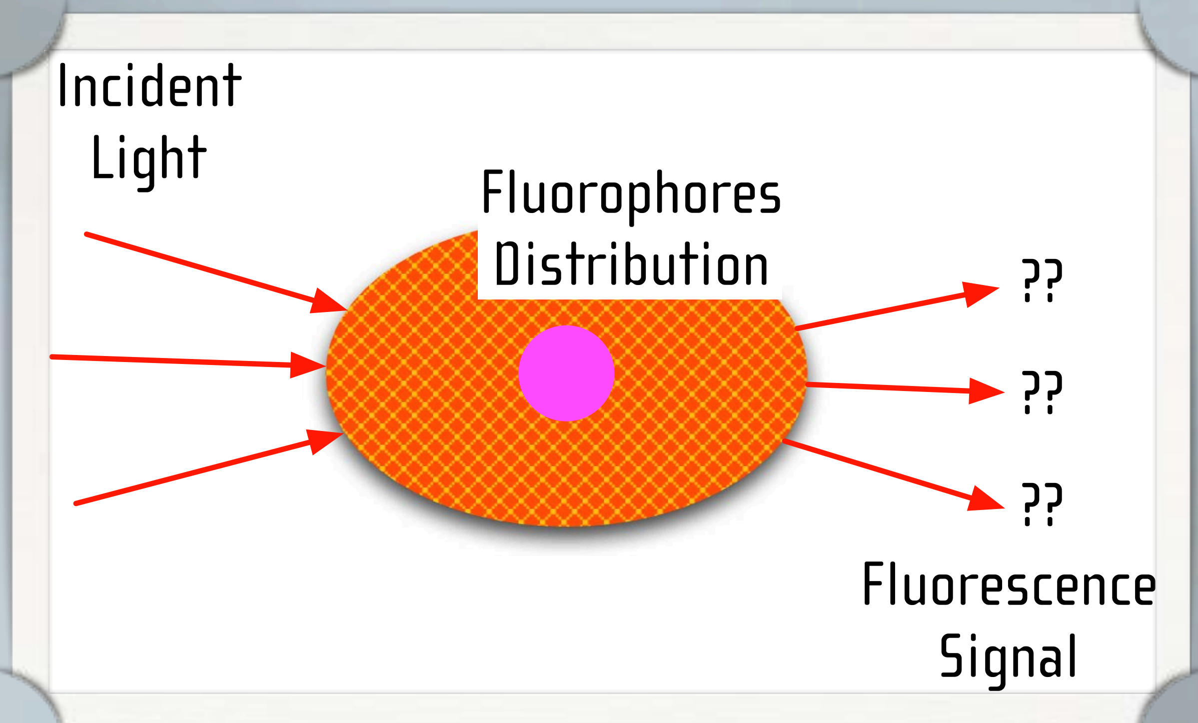

Forward Solver

- Monte Carlo (MC) is the gold standard,
- Diffusion Approximation (DA),
- Radiative Transfer Equation (RTE) is still under investigation.

The Inverse Problem in Fluorescence Molecular Imaging

The **inverse problem** in fluorescence imaging is defined as the 3D reconstruction of a fluorophores distribution embedded into a turbid medium, like tissues, by utilizing the acquired fluorescence signal and the outcomes of the forward problem solution.

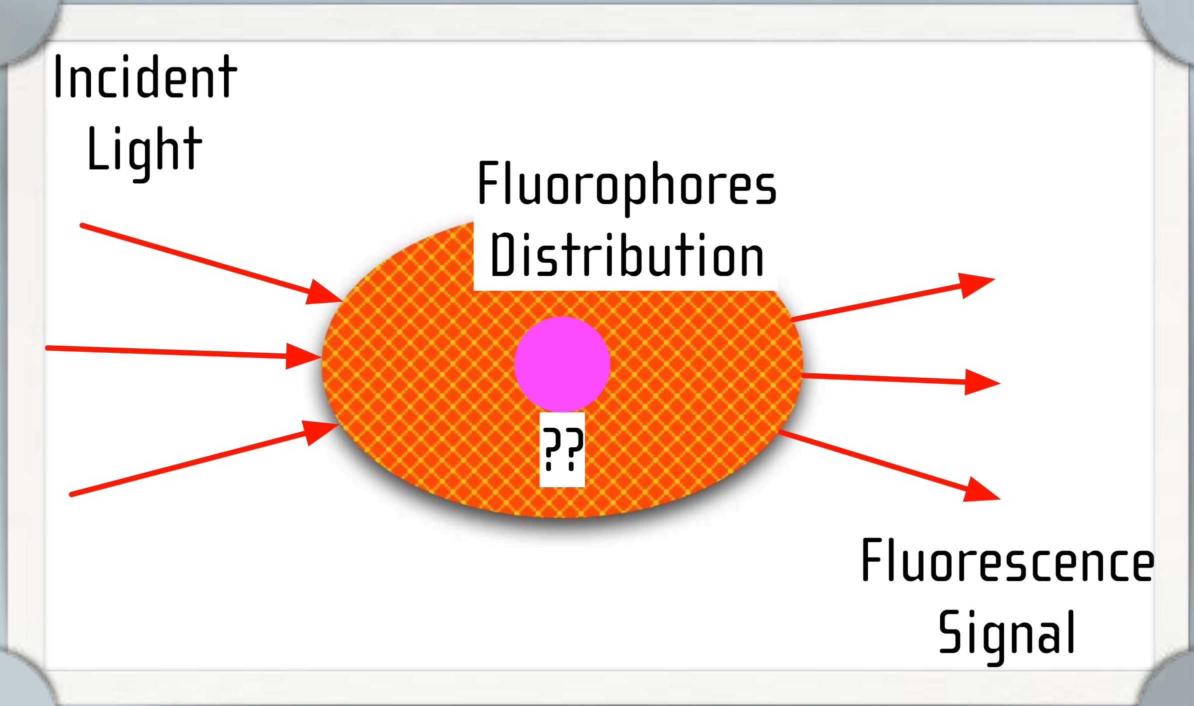

- Inverse Problem
  - Optimization problem is formed,
  - The fluorophores distribution is updated after each iteration,
  - Application of the forward solver to the new distribution,
  - Iterations continue until convergence occurs.

Applications of the Fluorescence Molecular Imaging

Example of current clinical application of the fluorescence molecular imaging

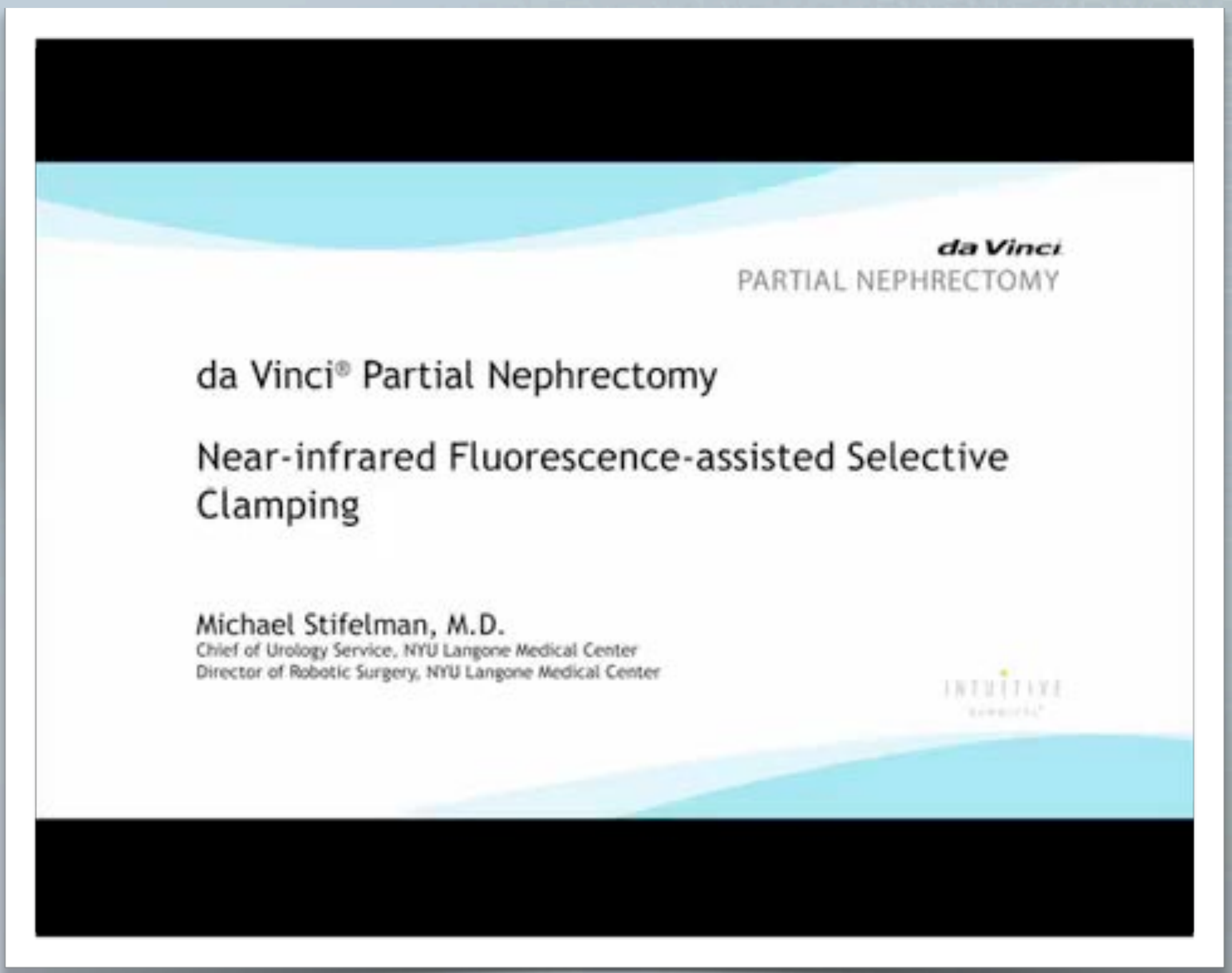

Applications of the Fluorescence Molecular Imaging

Example of fluorescence molecular imaging application in the pharmaceutical field.

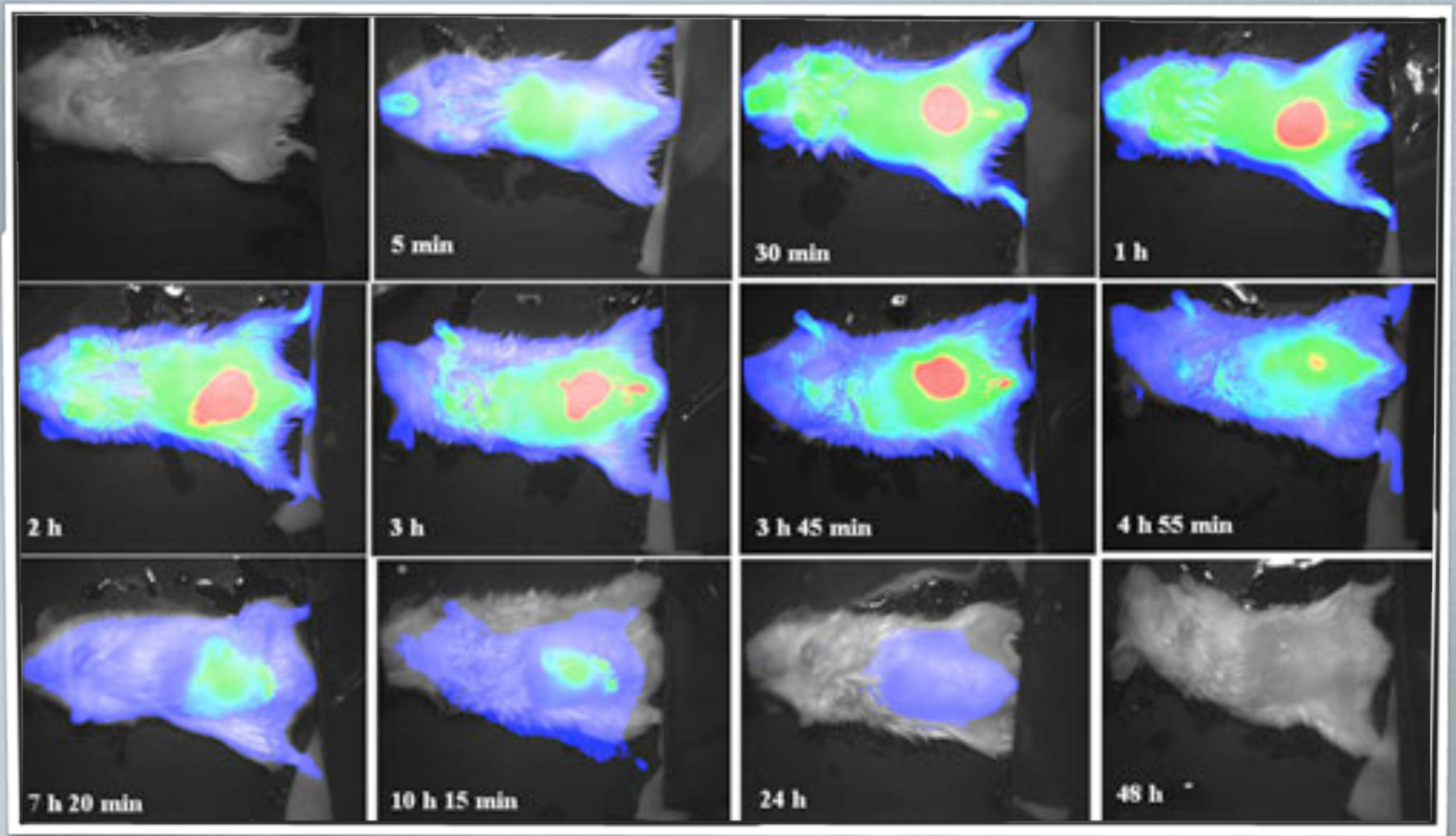

Kovar J et al., "A systematic approach to the development of fluorescent contrast agents for optical imaging of mouse cancer models", Cancer Res. 69(13):5592-600 (2009).

Applications of the Fluorescence Molecular Imaging

Possible prospects for clinical application of the fluorescence molecular imaging/tomography

- Breast cancer diagnosis.
- Tumor diagnosis/quantification.
- Photodynamic therapy evaluation.
- Lung inflammation.
- Immunology.
- Cardiology.

Outline

- The fluorescence phenomenon.
- Fluorescence molecular imaging – the problems.
- Image acquisition systems.
- Light propagation models.
- Conclusion.

Imaging Technologies

I. *In vivo* fluorescence microscopy

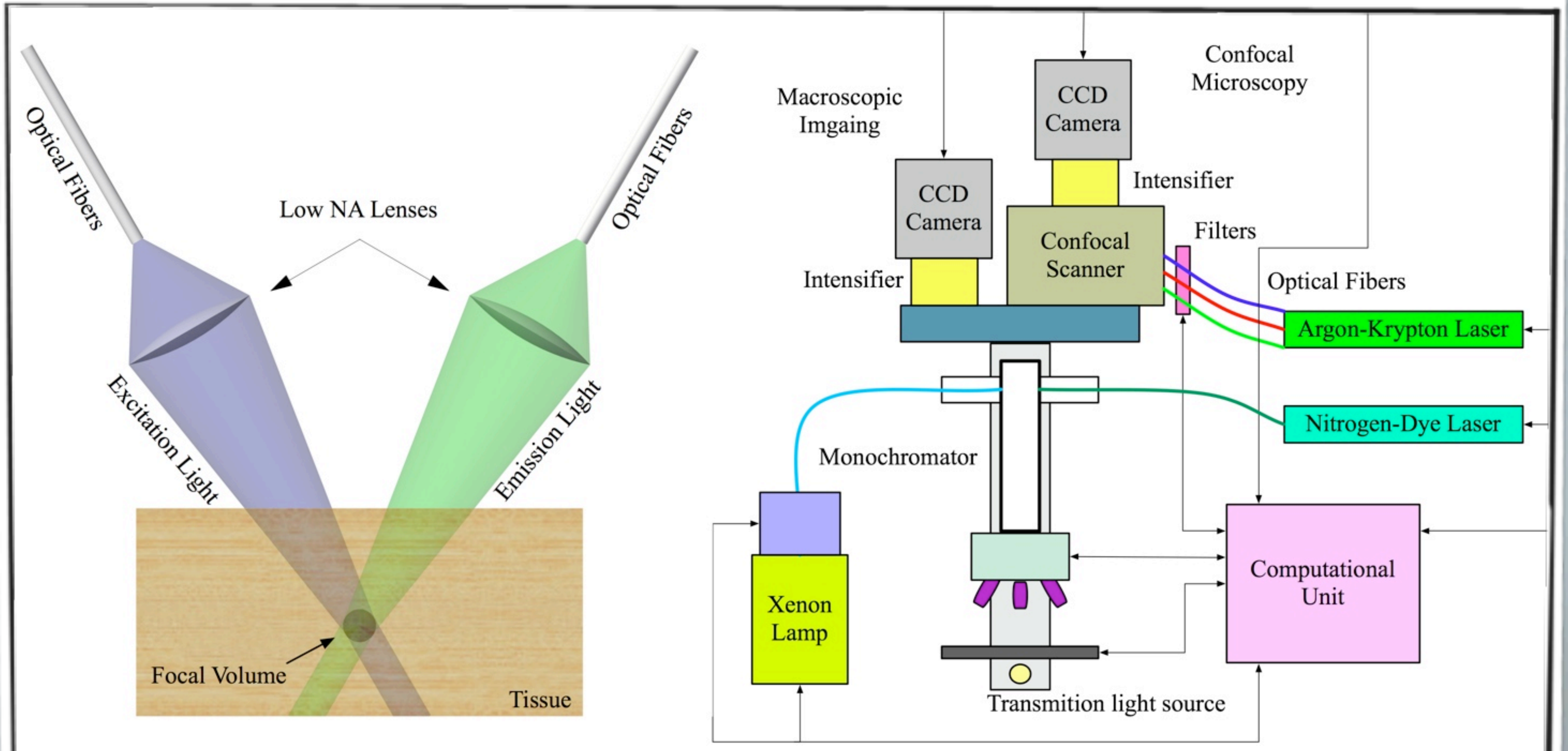

Falati S., Gross P., Merrill-Skoloff G., *et al.*, "*Real-Time in Vivo Imaging of Platelets, Tissue Factor and Fibrin During Arterial Thrombus Formation in the Mouse*", Nat Med, **8**(10):1175-1181 (2002).

Imaging Technologies

II. Epi-illumination imaging

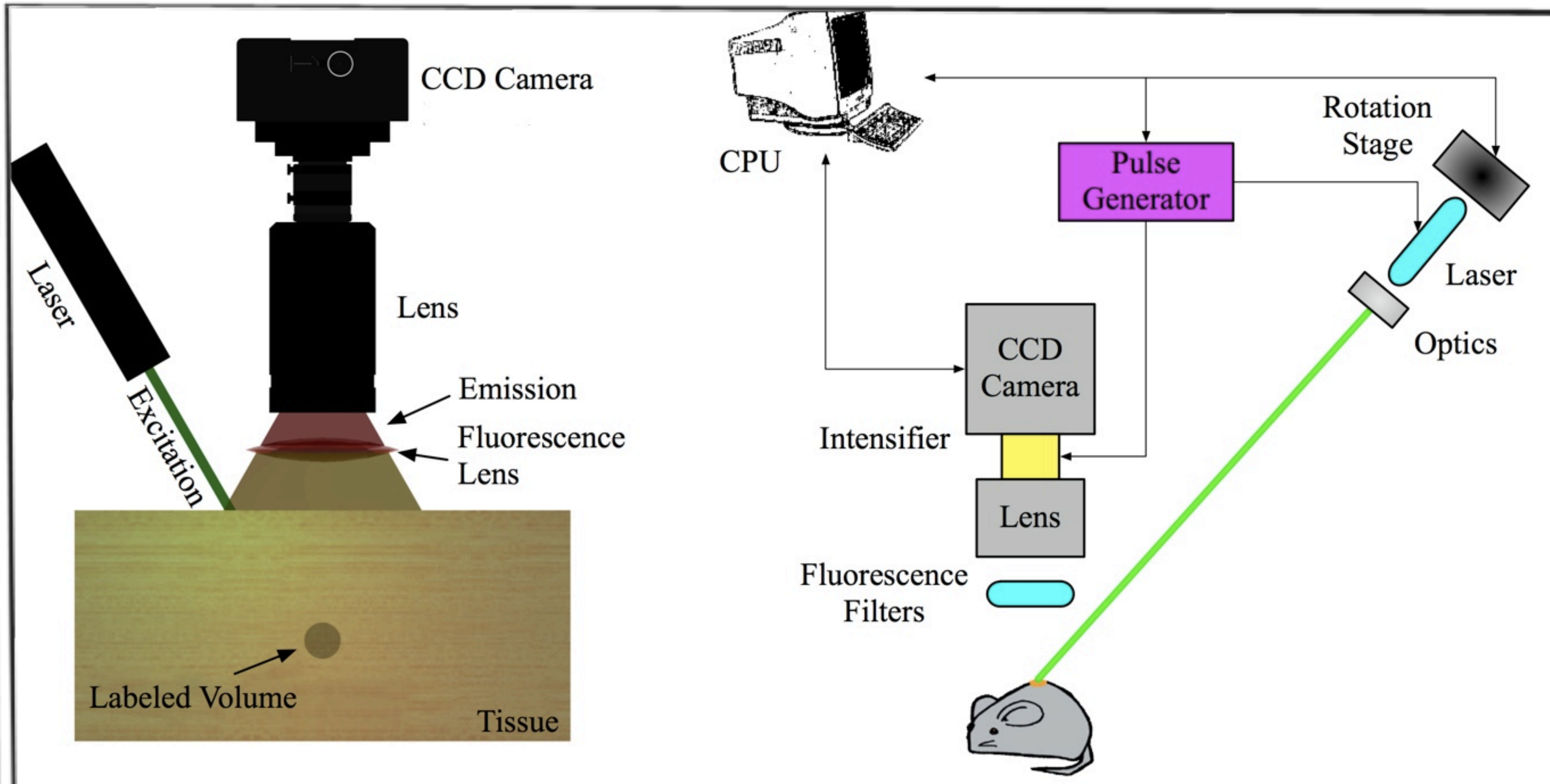

Joshi A., Bangerth W., Sharma R., *et al.*, "*Molecular Tomographic Imaging of Lymph Nodes wit Nir Fluorescence*", in 4th IEEE International Symposium on Biomedical Imaging: From Nano t Macro, IEEE Proc. 564-567 (2007).

Imaging Technologies

III.Trans-illumination imaging

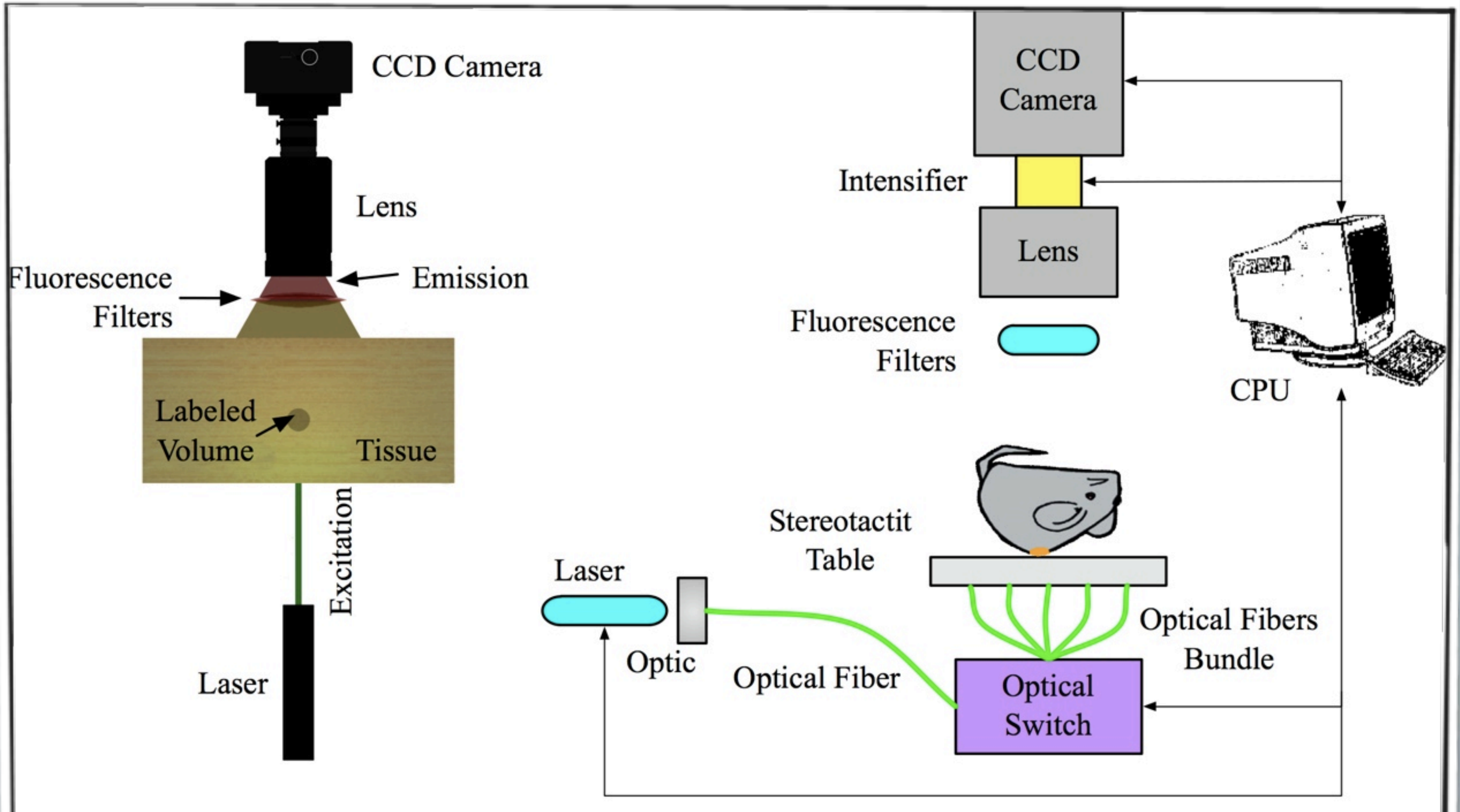

Schulz R.B., Ripoll J., Ntziachristos V., "*Noncontact Optical Tomography of Turbid Media*", Opt Lett, **28**(18):1701-1703 (2003).

Outline

- The fluorescence phenomenon.
- Fluorescence molecular imaging – the problems.
- Image acquisition systems.
- Light propagation models.
- Conclusion.

Light Propagation Models - Forward Problem Solution

- The Radiative Transfer Equation:
  - is accurate in predicting light propagation,
  - requires huge computing resources and
  - is time consuming.

$$\left.\begin{aligned}&\frac{i\cdot\omega}{c}\cdot I_{x/m}(\mathbf{r},\hat{\mathbf{s}})+\hat{\mathbf{s}}\cdot\nabla I_{x/m}(\mathbf{r},\hat{\mathbf{s}})+\left[\mu_{\alpha,x/m}(\mathbf{r})+\mu_{s,x/m}(\mathbf{r})\right]\cdot I_{x/m}(\mathbf{r},\hat{\mathbf{s}})\\&-\mu_{s,x/m}(\mathbf{r})\cdot\int_{4\pi}p_{x/m}(\hat{\mathbf{s}},\hat{\mathbf{s}}')\cdot I_{x/m}(\mathbf{r},\hat{\mathbf{s}}')\cdot d\hat{\mathbf{s}}'=\Lambda_{x/m}(\mathbf{r},\hat{\mathbf{s}})\end{aligned}\right|_{\mathbf{r}\in V_{RTE}}$$

$$I_{x/m}(\mathbf{r},\hat{\mathbf{s}})=\begin{cases}0 & \mathbf{r}\in S_{RTE,out}\setminus dS_{src},\ \hat{\mathbf{s}}\cdot\hat{\mathbf{n}}<0\\ I_{src}(\mathbf{r},\hat{\mathbf{s}}) & \mathbf{r}\in dS_{src},\ \hat{\mathbf{s}}\cdot\hat{\mathbf{n}}<0\end{cases}$$

- The Diffusion Approximation:
  - is accurate in predicting light propagation when the application is scattered dominated,
  - provides inaccurate predictions close to the light source and
  - provides inaccurate predictions close to the region boundaries.

$$\left.\frac{i\cdot\omega}{c}\cdot U_{x/m}(\mathbf{r})-\nabla\left[D_{x/m}(\mathbf{r})\cdot\nabla U_{x/m}(\mathbf{r})\right]+\mu_{\alpha,x/m}(\mathbf{r})\cdot U_{x/m}(\mathbf{r})=\Lambda_{0,x/m}(\mathbf{r})\right|_{\mathbf{r}\in V_{DA}}$$

$$U_{x/m}(\mathbf{r})=-2\cdot A\cdot D_{x/m}(\mathbf{r})\cdot\frac{\partial}{\partial\hat{\mathbf{n}}}U_{x/m}(\mathbf{r})\qquad \mathbf{r}\in S_{DA,out},\ \hat{\mathbf{s}}\cdot\hat{\mathbf{n}}<0$$

Light Propagation Models – Forward Problem Solution

Dual Coupled RTE-DA model

RTE

$$\left.\begin{aligned}&\frac{i\cdot\omega}{c}\cdot I_{x/m}(\mathbf{r},\hat{\mathbf{s}})+\hat{\mathbf{s}}\cdot\nabla I_{x/m}(\mathbf{r},\hat{\mathbf{s}})+\left[\mu_{\alpha,x/m}(\mathbf{r})+\mu_{s,x/m}(\mathbf{r})\right]\cdot I_{x/m}(\mathbf{r},\hat{\mathbf{s}})\\&-\mu_{s,x/m}(\mathbf{r})\cdot\int_{4\pi}p_{x/m}(\hat{\mathbf{s}},\hat{\mathbf{s}}')\cdot I_{x/m}(\mathbf{r},\hat{\mathbf{s}}')\cdot d\hat{\mathbf{s}}'=\Lambda_{x/m}(\mathbf{r},\hat{\mathbf{s}})\end{aligned}\right|_{\mathbf{r}\in V_{RTE}}$$

Vacuum boundary condition

$$I_{x/m}(\mathbf{r},\hat{\mathbf{s}})=\begin{cases}0 & \mathbf{r}\in S_{RTE,out}\setminus dS_{src},\ \hat{\mathbf{s}}\cdot\hat{\mathbf{n}}<0\\ I_{src}(\mathbf{r},\hat{\mathbf{s}}) & \mathbf{r}\in dS_{src},\ \hat{\mathbf{s}}\cdot\hat{\mathbf{n}}<0\end{cases}$$

Interface boundary condition

$$\left.I_{x/m}(\mathbf{r},\hat{\mathbf{s}})=U_{x/m}(\mathbf{r})-\frac{3}{4\cdot\pi}\cdot\left[D_{x/m}(\mathbf{r})\cdot\nabla U_{x/m}(\mathbf{r})\right]\cdot\hat{\mathbf{s}}\right|_{\mathbf{r}\in S_{interface}}$$

DA

$$\left.\frac{i\cdot\omega}{c}\cdot U_{x/m}(\mathbf{r})-\nabla\left[D_{x/m}(\mathbf{r})\cdot\nabla U_{x/m}(\mathbf{r})\right]+\mu_{\alpha,x/m}(\mathbf{r})\cdot U_{x/m}(\mathbf{r})=\Lambda_{0,x/m}(\mathbf{r})\right|_{\mathbf{r}\in V_{DA}}$$

Robin type boundary condition

$$U_{x/m}(\mathbf{r})=-2\cdot A\cdot D_{x/m}(\mathbf{r})\cdot\frac{\partial}{\partial\hat{\mathbf{n}}}U_{x/m}(\mathbf{r})\qquad \mathbf{r}\in S_{DA,out},\ \hat{\mathbf{s}}\cdot\hat{\mathbf{n}}<0$$

Interface boundary condition

$$U_{x/m}(\mathbf{r})=\frac{1}{4\cdot\pi}\cdot\int_{4\pi}I_{x/m}(\mathbf{r},\hat{\mathbf{s}})\cdot d\hat{\mathbf{s}}\qquad \mathbf{r}\in S_{interface}$$

Light Propagation Models – Forward Problem Solution

Dual Coupled RTE-DA model

RTE

$$\left.\begin{aligned}&\frac{i\cdot\omega}{c}\cdot I_{x/m}(\mathbf{r},\hat{\mathbf{s}})+\hat{\mathbf{s}}\cdot\nabla I_{x/m}(\mathbf{r},\hat{\mathbf{s}})+\left[\mu_{\alpha,x/m}(\mathbf{r})+\mu_{s,x/m}(\mathbf{r})\right]\cdot I_{x/m}(\mathbf{r},\hat{\mathbf{s}})\\&-\mu_{s,x/m}(\mathbf{r})\cdot\int_{4\pi}p_{x/m}(\hat{\mathbf{s}},\hat{\mathbf{s}}')\cdot I_{x/m}(\mathbf{r},\hat{\mathbf{s}}')\cdot d\hat{\mathbf{s}}'=\Lambda_{x/m}(\mathbf{r},\hat{\mathbf{s}})\end{aligned}\right|_{\mathbf{r}\in V_{RTE}}$$

Vacuum boundary condition

$$I_{x/m}(\mathbf{r},\hat{\mathbf{s}})=\begin{cases}0 & \mathbf{r}\in S_{RTE,out}\setminus dS_{src},\ \hat{\mathbf{s}}\cdot\hat{\mathbf{n}}<0\\ I_{src}(\mathbf{r},\hat{\mathbf{s}}) & \mathbf{r}\in dS_{src},\end{cases}$$

$$\Lambda_x(\mathbf{r},\hat{\mathbf{s}})=\Lambda_{0,x}(\mathbf{r})=0$$

$$\Lambda_m(\mathbf{r},\hat{\mathbf{s}})=\Lambda_{0,m}(\mathbf{r})=\frac{\eta\cdot\mu_{\alpha,x}^{fluo}(\mathbf{r})}{1+i\cdot\omega\cdot\tau(\mathbf{r})}\cdot U_x(\mathbf{r})$$

Interface boundary condition

$$I_{x/m}(\mathbf{r},\hat{\mathbf{s}})=U_{x/m}(\mathbf{r})-\frac{3}{4\cdot\pi}\cdot\left[D_{x/m}(\mathbf{r})\cdot\nabla\right.$$

DA

$$\left.\frac{i\cdot\omega}{c}\cdot U_{x/m}(\mathbf{r})-\nabla\left[D_{x/m}(\mathbf{r})\cdot\nabla U_{x/m}(\mathbf{r})\right]+\mu_{\alpha,x/m}(\mathbf{r})\cdot U_{x/m}(\mathbf{r})=\Lambda_{0,x/m}(\mathbf{r})\right|_{\mathbf{r}\in V_{DA}}$$

Robin type boundary condition

$$U_{x/m}(\mathbf{r})=-2\cdot A\cdot D_{x/m}(\mathbf{r})\cdot\frac{\partial}{\partial\hat{\mathbf{n}}}U_{x/m}(\mathbf{r})\qquad \mathbf{r}\in S_{DA,out},\ \hat{\mathbf{s}}\cdot\hat{\mathbf{n}}<0$$

Interface boundary condition

$$U_{x/m}(\mathbf{r})=\frac{1}{4\cdot\pi}\cdot\int_{4\pi}I_{x/m}(\mathbf{r},\hat{\mathbf{s}})\cdot d\hat{\mathbf{s}}\qquad \mathbf{r}\in S_{interface}$$

Light Propagation Models - Forward Problem Solution

Dual Coupled RTE-DA model

RTE

$$\left.\begin{aligned}&\frac{i\cdot\omega}{c}\cdot I_{x/m}(\mathbf{r},\hat{\mathbf{s}})+\hat{\mathbf{s}}\cdot\nabla I_{x/m}(\mathbf{r},\hat{\mathbf{s}})+\left[\mu_{\alpha,x/m}(\mathbf{r})+\mu_{s,x/m}(\mathbf{r})\right]\cdot I_{x/m}(\mathbf{r},\hat{\mathbf{s}})\\&-\mu_{s,x/m}(\mathbf{r})\cdot\int_{4\pi}p_{x/m}(\hat{\mathbf{s}},\hat{\mathbf{s}}')\cdot I_{x/m}(\mathbf{r},\hat{\mathbf{s}}')\cdot d\hat{\mathbf{s}}'=\Lambda_{x/m}(\mathbf{r},\hat{\mathbf{s}})\end{aligned}\right|_{\mathbf{r}\in V_{RTE}}$$

Vacuum boundary condition

$$I_{x/m}(\mathbf{r},\hat{\mathbf{s}})=\begin{cases}0 & \mathbf{r}\in S_{RTE,out}\setminus dS_{src},\ \hat{\mathbf{s}}\cdot\hat{\mathbf{n}}<0\\ I_{src}(\mathbf{r},\hat{\mathbf{s}}) & \mathbf{r}\in dS_{src},\ \ldots\end{cases}$$

$$\Lambda_x(\mathbf{r},\hat{\mathbf{s}})=\Lambda_{0,x}(\mathbf{r})=0$$

$$\Lambda_m(\mathbf{r},\hat{\mathbf{s}})=\Lambda_{0,m}(\mathbf{r})=\frac{\eta\cdot\mu_{\alpha,x}^{fluo}(\mathbf{r})}{1+i\cdot\omega\cdot\tau(\mathbf{r})}\cdot U_x(\mathbf{r})$$

Interface boundary condition

$$\mu_{s,x/m}(\mathbf{r})=\mu_{s,x/m}^{tis}(\mathbf{r})$$

$$\mu_{\alpha,x/m}(\mathbf{r})=\mu_{\alpha,x/m}^{tis}(\mathbf{r})+\mu_{\alpha,x/m}^{fluo}(\mathbf{r})$$

$$\ldots\cdot\left[D_{x/m}(\mathbf{r})\cdot\nabla\ldots\right.\quad\ldots_{interface}$$

DA

$$\left.\frac{i\cdot\omega}{c}\cdot U_{x/m}(\mathbf{r})-\nabla\left[D_{x/m}(\mathbf{r})\cdot\nabla U_{x/m}(\mathbf{r})\right]+\mu_{\alpha,x/m}(\mathbf{r})\cdot U_{x/m}(\mathbf{r})=\Lambda_{0,x/m}(\mathbf{r})\right|_{\mathbf{r}\in V_{DA}}$$

Robin type boundary condition

$$U_{x/m}(\mathbf{r})=-2\cdot A\cdot D_{x/m}(\mathbf{r})\cdot\frac{\partial}{\partial\hat{\mathbf{n}}}U_{x/m}(\mathbf{r})\qquad \mathbf{r}\in S_{DA,out},\ \hat{\mathbf{s}}\cdot\hat{\mathbf{n}}<0$$

Interface boundary condition

$$U_{x/m}(\mathbf{r})=\frac{1}{4\cdot\pi}\cdot\int_{4\pi}I_{x/m}(\mathbf{r},\hat{\mathbf{s}})\cdot d\hat{\mathbf{s}}\qquad \mathbf{r}\in S_{interface}$$

The Dual Coupled RTE-DA Model

Numerical solution of the forward problem

The finite elements method is the one adopted as the numerical solution approximation of the forward problem in fluorescence molecular imaging.

The Dual Coupled RTE-DA Model

Numerical solution of the forward problem

- Variational formulation of the dual coupled RTE-DA model.
  - RTE is multiplied with the test function $\psi(\mathbf{r},\hat{\mathbf{s}})$ and integrated over the domain V_{RTE} and for all the angular directions.
  - DA is multiplied with the test function $y(\mathbf{r})$ and integrated over the domain V_{DA}.

- Finite elements approximation of the dual coupled RTE-DA model.
  - The solutions of the variational formulation are approximated in piece-wise linear functions per element (standard Galerkin technique).

$$I_{x/m}(\mathbf{r},\hat{\mathbf{s}}) \approx I^{h}_{x/m}(\mathbf{r},\hat{\mathbf{s}}) = \sum_{i=1}^{N_n}\sum_{l=1}^{N_a}\alpha_{il,x/m}\cdot\psi_i(\mathbf{r})\cdot\psi_l(\hat{\mathbf{s}})$$

$$U_{x/m}(\mathbf{r}) \approx U^{h}_{x/m}(\mathbf{r}) = \sum_{k=1}^{N} a_{k,x/m}\cdot y_k(\mathbf{r})$$

The Dual Coupled RTE-DA Model

Numerical solution of the forward problem

- Application of the streamline diffusion modification, sdm, for minimization of the “photon rays”.

$$\psi(\mathbf{r},\hat{\mathbf{s}}) := \psi(\mathbf{r},\hat{\mathbf{s}}) + \delta(\mathbf{r}) \cdot \hat{\mathbf{s}} \cdot \nabla\psi(\mathbf{r},\hat{\mathbf{s}})$$

- Transformation of the resulted linear algebraic system into its matrix formalism.

$$\begin{bmatrix} \mathbf{A}_{\mathrm{RTE},x/m} & \mathbf{B}_{\mathrm{RTE},x/m} \\ \mathbf{B}_{\mathrm{DA},x/m} & \mathbf{A}_{\mathrm{DA},x/m} \end{bmatrix} \cdot \begin{bmatrix} \boldsymbol{\alpha}_{x/m} \\ \mathbf{a}_{x/m} \end{bmatrix} = \begin{bmatrix} \mathbf{C}_{\mathrm{RTE},x/m} \\ \mathbf{C}_{\mathrm{DA},x/m} \end{bmatrix}$$

$$\mathbf{A}_{\mathrm{RTE},x/m}(h_1,h_2) = \mathbf{A}_0^{x/m}(h_1,h_2) + \mathbf{A}_1^{x/m}(h_1,h_2) + \mathbf{A}_2^{x/m}(h_1,h_2) + \mathbf{A}_3^{x/m}(h_1,h_2) + \mathbf{A}_4^{x/m}(h_1,h_2)$$

$$\mathbf{A}_{\mathrm{DA},x/m}(p,k) = \mathbf{Ke}_{x/m}(p,k) + \mathbf{Me}_{x/m}(p,k) + \mathbf{Pe}_{x/m}(p,k)$$

The Dual Coupled RTE-DA Model

Numerical solution of the forward problem

- Application of the streamline diffusion modification, sdm, for minimization of the "photon rays".

- Transl… matri…

$$\mathbf{A}_0^{x/m}\left(h_1,h_2\right)=\frac{i\cdot\omega}{c}\cdot\int_{V_{RTE}}\psi_i\left(\mathbf{r}\right)\cdot\psi_j\left(\mathbf{r}\right)\cdot d\mathbf{r}\cdot\int_{4\pi}\psi_l\left(\hat{\mathbf{s}}\right)\cdot\psi_q\left(\hat{\mathbf{s}}\right)\cdot d\hat{\mathbf{s}}$$

$$+\frac{i\cdot\omega}{c}\cdot\int_{V_{RTE}}\int_{4\pi}\delta_{x/m}\left(\mathbf{r}\right)\cdot\hat{\mathbf{s}}\cdot\nabla\psi_j\left(\mathbf{r}\right)\cdot\psi_q\left(\hat{\mathbf{s}}\right)\cdot\psi_l\left(\hat{\mathbf{s}}\right)\cdot d\hat{\mathbf{s}}\cdot\psi_i\left(\mathbf{r}\right)\cdot d\mathbf{r}$$

$$\begin{bmatrix}\mathbf{B}_{DA,x/m} & \mathbf{A}_{DA,x/m}\end{bmatrix}\begin{bmatrix}\mathbf{a}_{x/m}\end{bmatrix}\begin{bmatrix}\mathbf{C}_{DA,x/m}\end{bmatrix}$$

$$\mathbf{A}_{RTE,x/m}\left(h_1,h_2\right)=\mathbf{A}_0^{x/m}\left(h_1,h_2\right)+\mathbf{A}_1^{x/m}\left(h_1,h_2\right)+\mathbf{A}_2^{x/m}\left(h_1,h_2\right)+\mathbf{A}_3^{x/m}\left(h_1,h_2\right)+\mathbf{A}_4^{x/m}\left(h_1,h_2\right)$$

$$\mathbf{A}_{DA,x/m}\left(p,k\right)=\mathbf{Ke}_{x/m}\left(p,k\right)+\mathbf{Me}_{x/m}\left(p,k\right)+\mathbf{Pe}_{x/m}\left(p,k\right)$$

The Dual Coupled RTE-DA Model

Numerical solution of the forward problem

- Application of the streamline diffusion modification, sdm, for minimization of the "photon rays".

$$\psi(\mathbf{r},\hat{\mathbf{s}}) := \psi(\mathbf{r},\hat{\mathbf{s}}) + \delta(\mathbf{r})\cdot\hat{\mathbf{s}}\cdot\nabla\psi(\mathbf{r},\hat{\mathbf{s}})$$

- Transformation of the resulted linear algebraic system into its matrix formalism.

$$\begin{bmatrix} \mathbf{A}_{\mathrm{RTE,x/m}} & \mathbf{B}_{\mathrm{RTE,x/m}} \end{bmatrix} \begin{bmatrix} \boldsymbol{\alpha}_{\mathrm{x/m}} \end{bmatrix} = \begin{bmatrix} \mathbf{C}_{\mathrm{RTE,x/m}} \end{bmatrix}$$

$$\mathbf{Ke}_{\mathrm{x/m}}(\mathrm{p,k}) = \frac{\mathrm{i}\cdot\omega}{c}\cdot\int_{V_{DA}} y_k(\mathbf{r})\cdot y_p(\mathbf{r})\cdot d\mathbf{r} + \int_{V_{DA}} \mu_{\alpha,\mathrm{x/m}}(\mathbf{r})\cdot y_k(\mathbf{r})\cdot y_p(\mathbf{r})\cdot d\mathbf{r}$$

$$\mathbf{A}_{\mathrm{RTE,x/m}}(h_1,h_2) = \mathbf{A}_0^{\mathrm{x/m}}(h_1,h_2) + \mathbf{A}_1^{\mathrm{x/m}}(h_1,h_2) + \mathbf{A}_2^{\mathrm{x/m}}(h_1,h_2) + \mathbf{A}_3^{\mathrm{x/m}}(h_1,h_2) + \mathbf{A}_4^{\mathrm{x/m}}(h_1,h_2)$$

$$\mathbf{A}_{\mathrm{DA,x/m}}(\mathrm{p,k}) = \mathbf{Ke}_{\mathrm{x/m}}(\mathrm{p,k}) + \mathbf{Me}_{\mathrm{x/m}}(\mathrm{p,k}) + \mathbf{Pe}_{\mathrm{x/m}}(\mathrm{p,k})$$

The Dual Coupled RTE-DA Model

Numerical solution of the forward problem

- Excitation solution and application of the outcomes for the solution of the emission.
  - The linear systems can be solved through application of the BiCGStab method.
- Spatial and angular integrals were confronted separately.
  - Assembly of the finite elements matrices with application of the Kronecker product.

$$\mathbf{C} = \mathbf{A} \otimes \mathbf{B} = \begin{bmatrix} a_{11} \cdot \mathbf{B} & \cdots & a_{n1} \cdot \mathbf{B} \\ \vdots & \ddots & \vdots \\ a_{1m} \cdot \mathbf{B} & \cdots & a_{nm} \cdot \mathbf{B} \end{bmatrix}$$

Gorpas D., Yova D., Politopoulos K., "A Three-dimensional Finite Elements Approach for the Coupled Radiative Transfer Equation and Diffusion Approximation Modeling in Fluorescence Imaging", J. Quant. Spectrosc. Radiat. Transfer, 111(4): 569-584 (2010).

Region Discretization

Discretization of the geometrical model

- Spatial discretization with application of the Delaunay triangulation method.

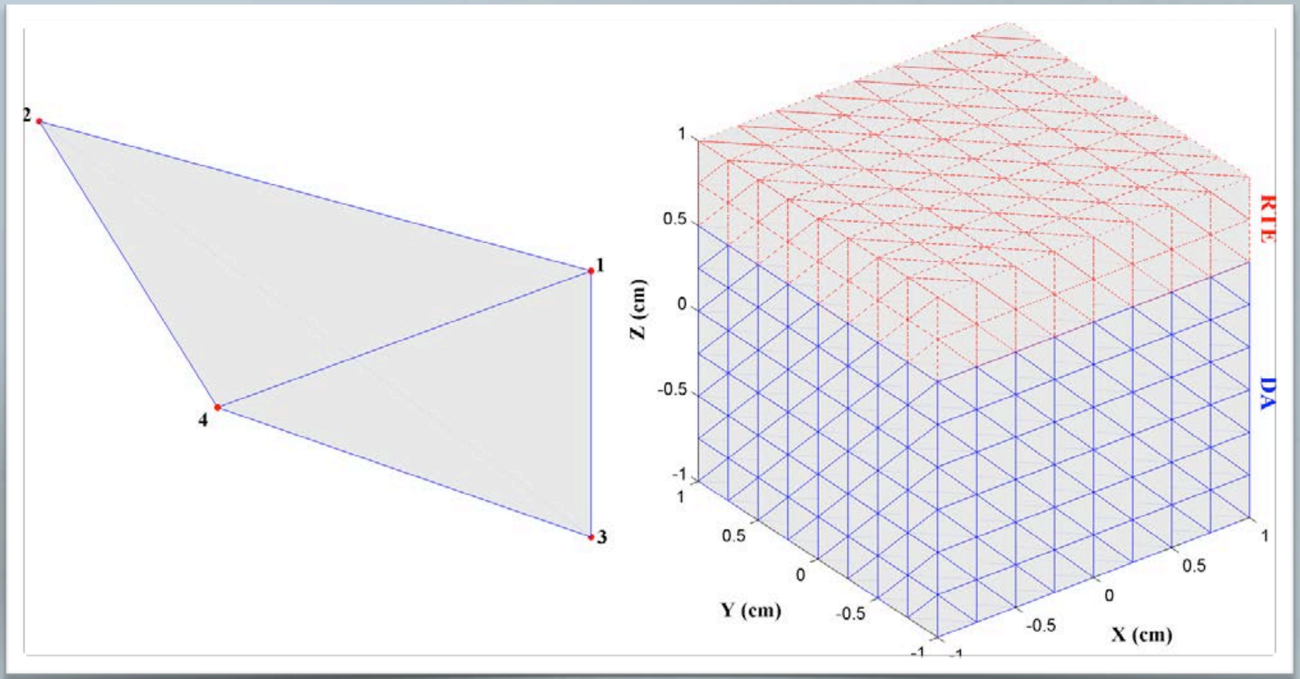

- Angular discretization with application of the Azimuthal technique.

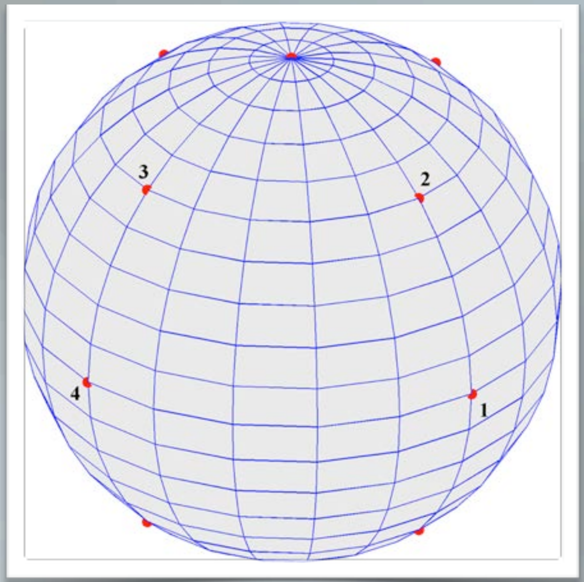

Super-Ellipsoidal Models

Optical properties distribution

- The volume optical properties distribution was implemented through application of the super-ellipsoidal models.

$$f(x,y,z)=\left[\left(\frac{x}{a_1}\right)^{2/\varepsilon_2}+\left(\frac{y}{a_2}\right)^{2/\varepsilon_2}\right]^{\varepsilon_2/\varepsilon_1}+\left(\frac{z}{a_3}\right)^{2/\varepsilon_1}$$

- Description of the position of a three-dimensional point, related to the super-ellipsoid surface.
  - f(x,y,z)=1 when the point is located on the super-ellipsoid surface,
  - f(x,y,z)<1 when the point is located inside the super-ellipsoid model and
  - f(x,y,z)>1 when the point is located outside the super-ellipsoid model.

- Spatial distribution of the absorption coefficient.

$$\mu_{\alpha,x/m}(\mathbf{r})=\mu^{tis}_{\alpha,x/m}+q(\mathbf{r})\cdot\mu^{fluo}_{\alpha,x/m} \qquad q(\mathbf{r})=\begin{cases}1, f(x,y,z)\le 1\\ 0, f(x,y,z)>1\end{cases}$$

Super-Ellipsoidal Models

Optical properties distribution

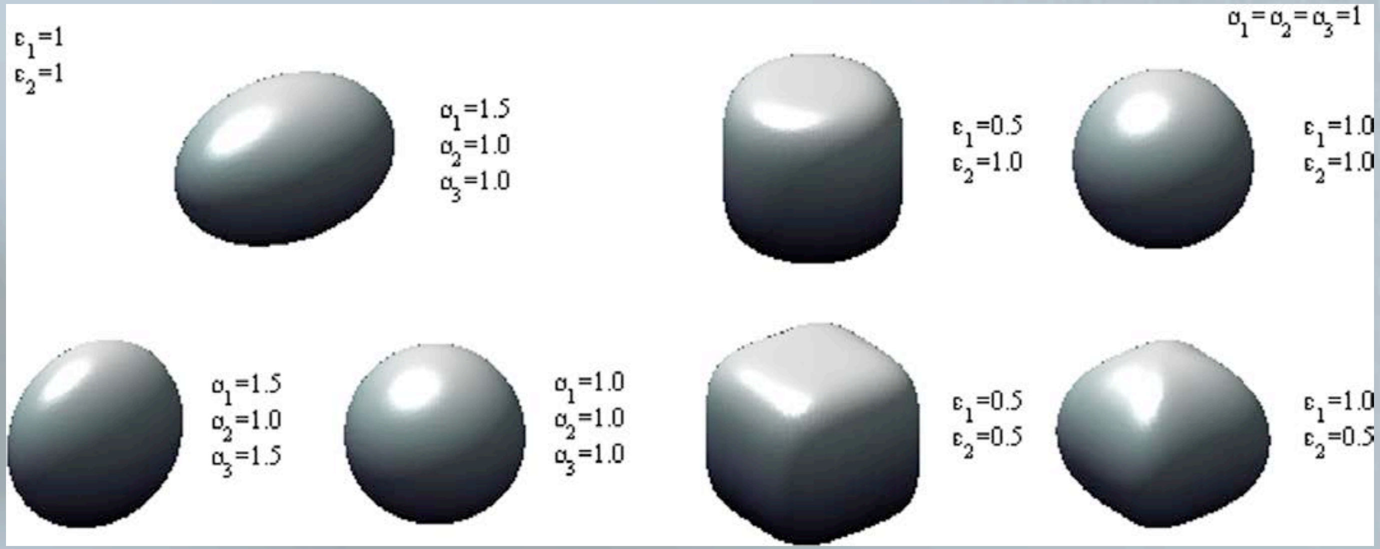

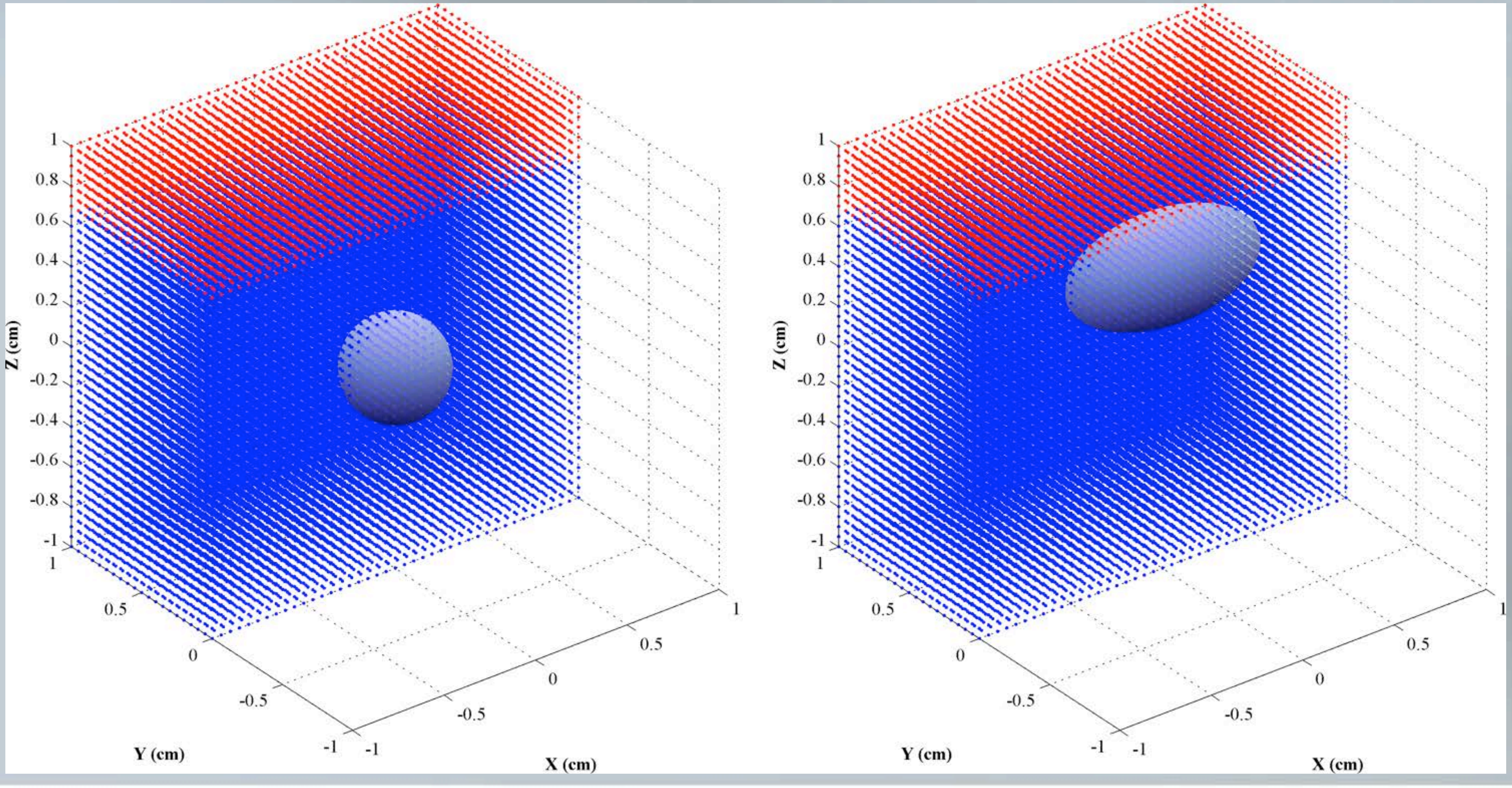

Evaluation in Frequency Domain

Results in the frequency domain

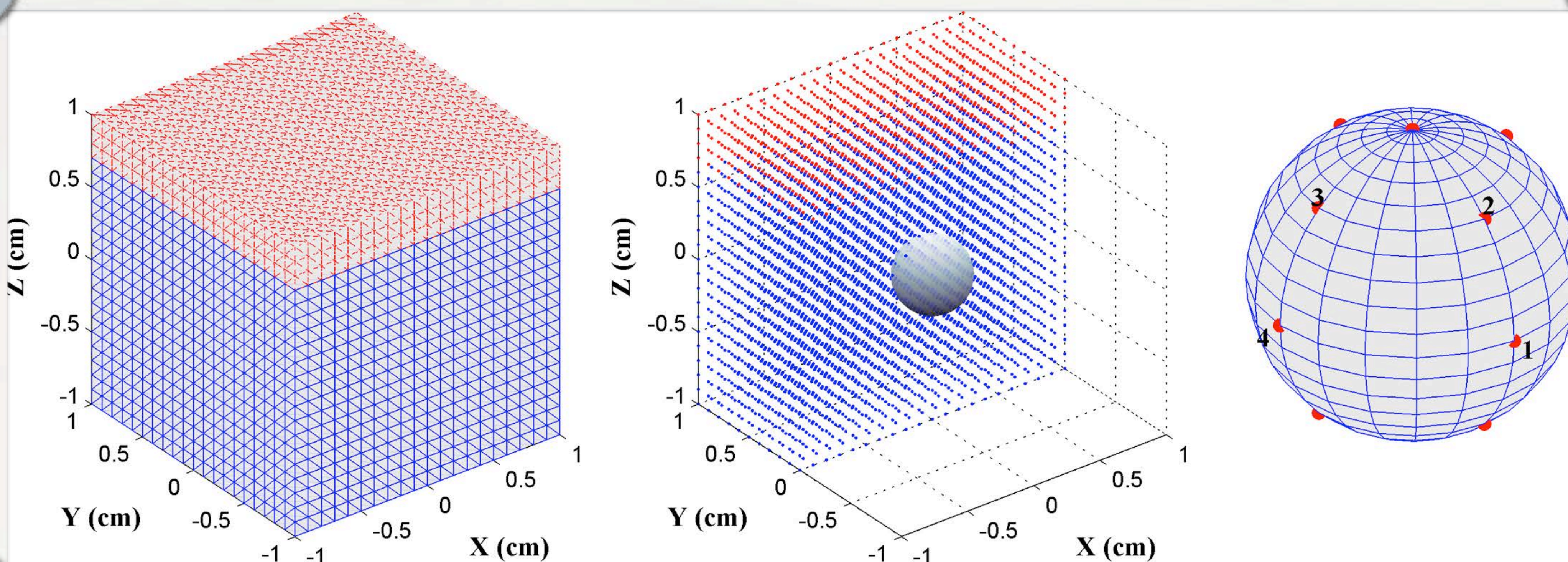

Evaluation in Frequency Domain

Results in the frequency domain

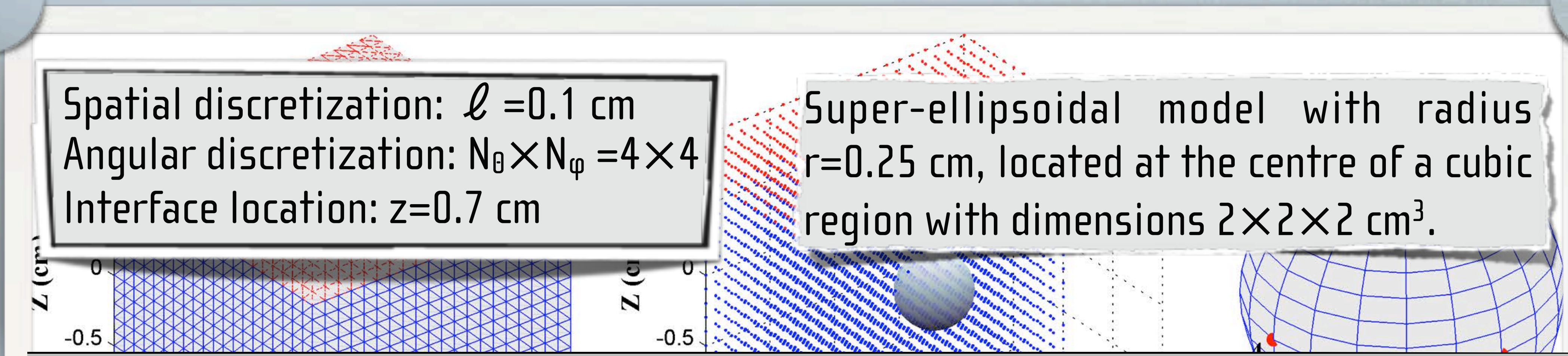

Spatial discretization: ℓ =0.1 cm
Angular discretization: $N_\theta \times N_\varphi = 4 \times 4$
Interface location: z=0.7 cm

Super-ellipsoidal model with radius r=0.25 cm, located at the centre of a cubic region with dimensions $2 \times 2 \times 2$ cm^3.

	DA	RTE	RTE-DA
Tetrahedral Elements	48000	48000	7200-RTE 40800-DA
Nodal Points	9261	9261	1764-RTE 7938-DA
Angular Elements	-	16	16-RTE
Angular Nodes	-	20	20-RTE
Assembly Matrices Dimensions	[9261×9261]	[185220×185220]	[43218×43218]
Required Times (sec)	7.69	7.95	8.22

Evaluation in Frequency Domain

Results in the frequency domain

- Logarithm of the photon density modulation amplitude.

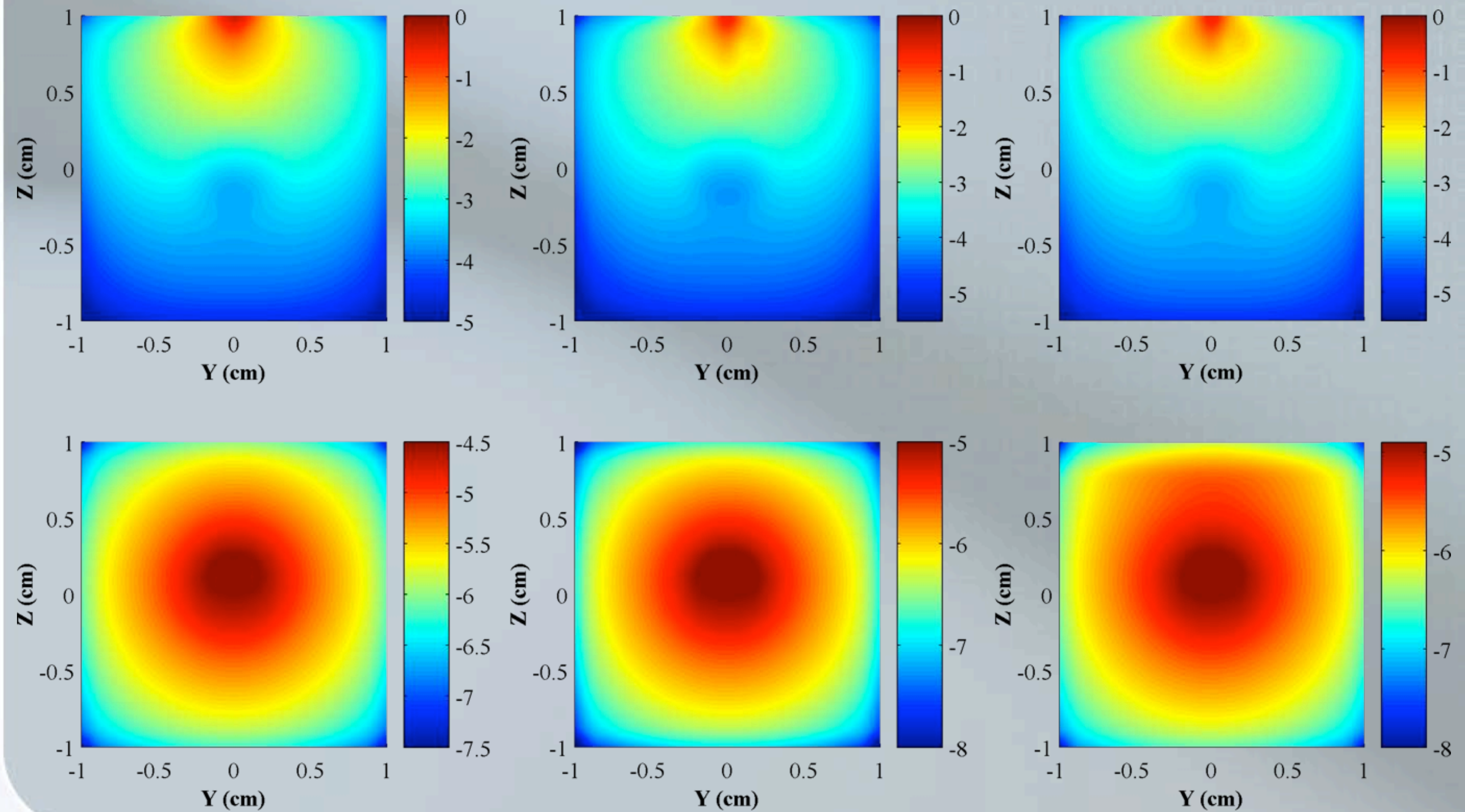

Evaluation in Frequency Domain

Results in the frequency domain

- Logarithm of the photon density modulation amplitude.

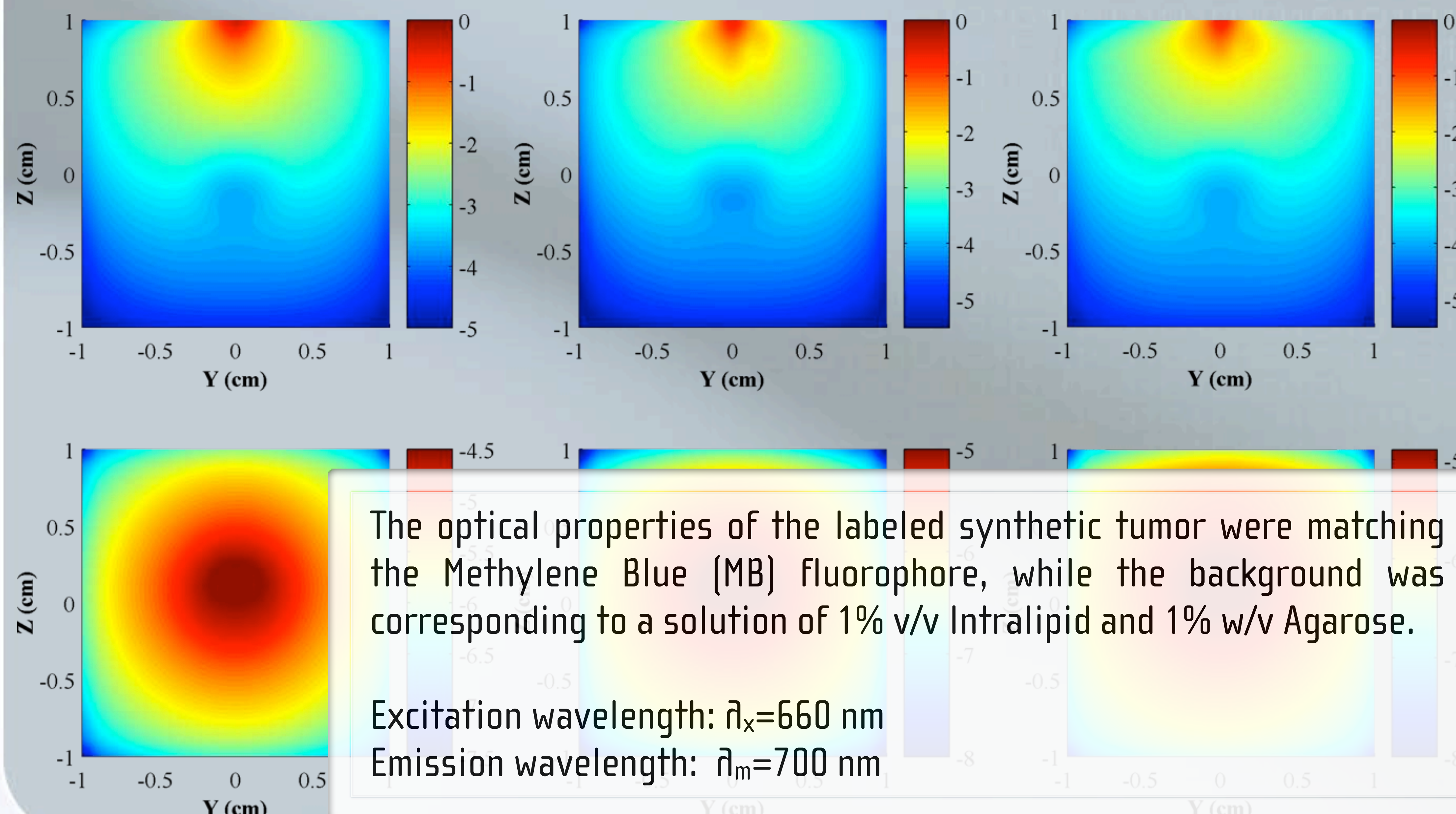

The optical properties of the labeled synthetic tumor were matching the Methylene Blue (MB) fluorophore, while the background was corresponding to a solution of 1% v/v Intralipid and 1% w/v Agarose.

Excitation wavelength: λ_x=660 nm
Emission wavelength: λ_m=700 nm

Evaluation in Frequency Domain

Results in the frequency domain

- Logarithm of the photon density modulation amplitude.

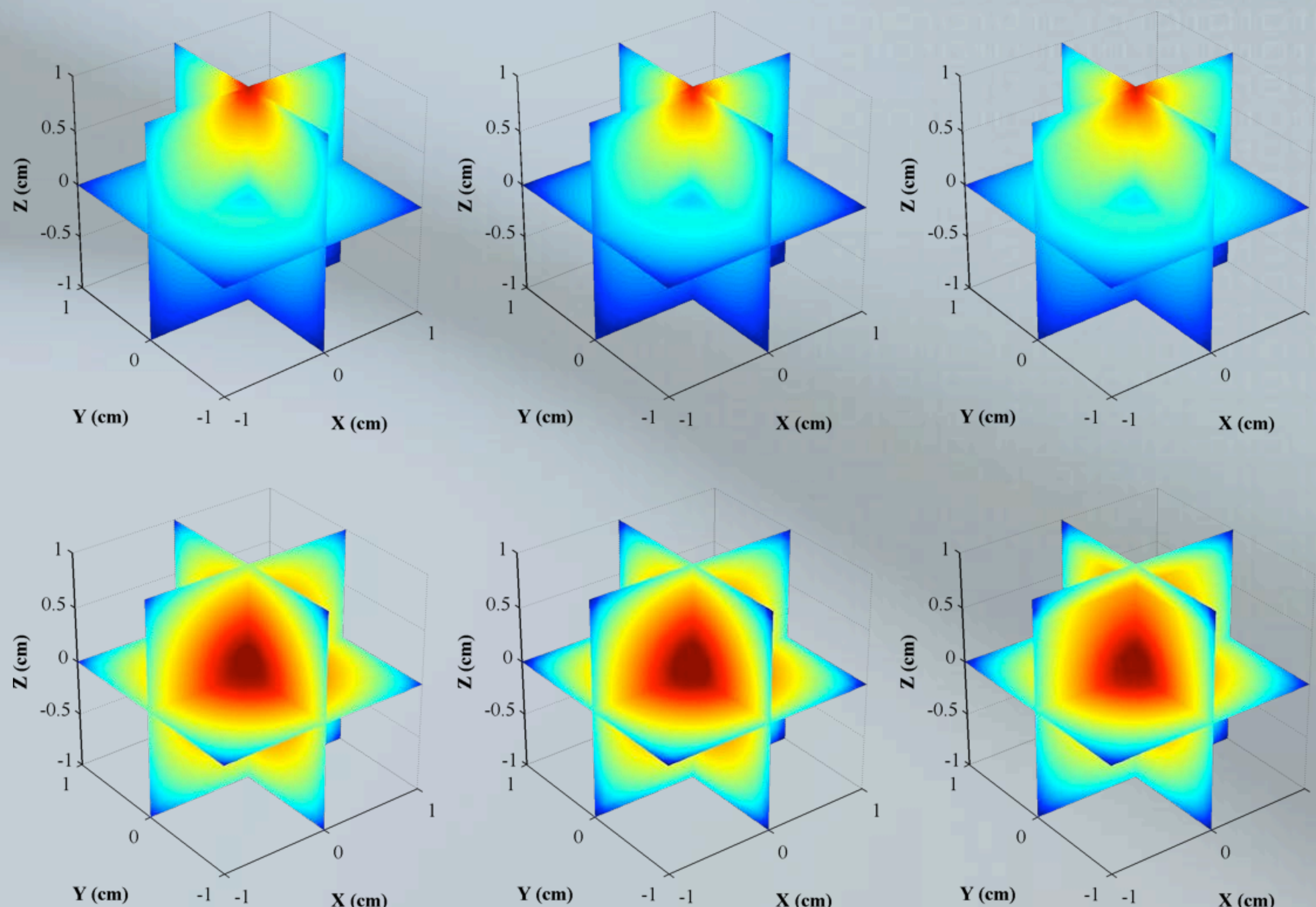

Evaluation in Frequency Domain

Results in the frequency domain

- Phase shift.

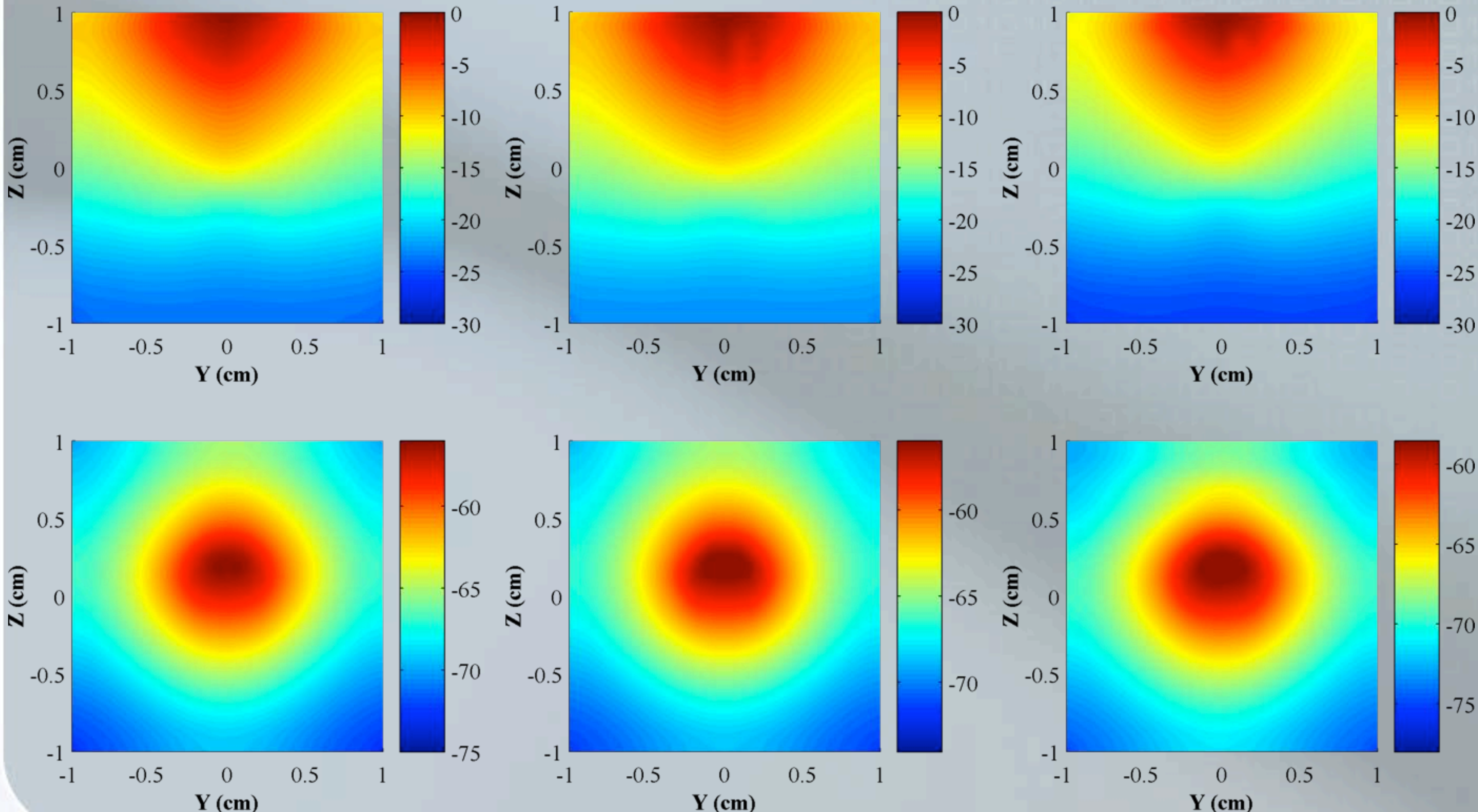

Evaluation in Frequency Domain

Results in the frequency domain

- Phase shift.

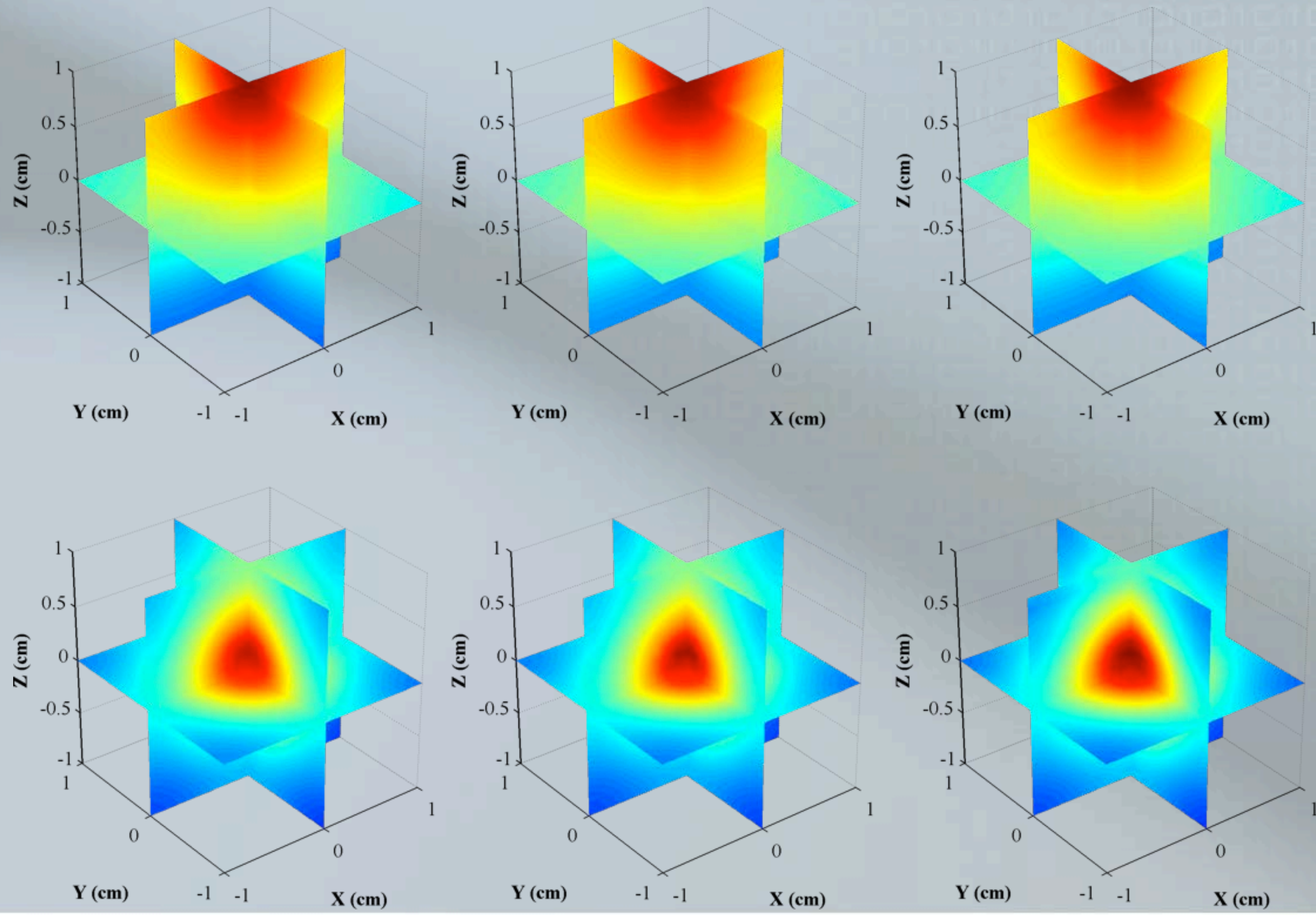

Evaluation in Frequency Domain

Evaluation of the results in the frequency domain

- Accuracy of the method.

Evaluation in Frequency Domain

Evaluation of the results in the frequency domain

- Accuracy of the method.
  - Estimated in regards to the RTE.

Evaluation in Frequency Domain

Evaluation of the results in the frequency domain

- Accuracy of the method.
  - Estimated in regards to the RTE.
  - Estimated through the absolute value of the relative error between the results of the dual coupled RTE-DA model and the RTE based model.

$$\mathrm{ARE}_{\mathrm{A}/\theta,\mathrm{DA/RTE-DA}} = \left| \frac{\mathrm{M}_{\mathrm{A}/\theta,\mathrm{RTE}} - \mathrm{M}_{\mathrm{A}/\theta,\mathrm{DA/RTE-DA}}}{\mathrm{M}_{\mathrm{A}/\theta,\mathrm{RTE}}} \right| \times 100\%$$

Evaluation in Frequency Domain

Evaluation of the results in the frequency domain

- Accuracy of the method.
  - Estimated in regards to the RTE.
  - Estimated through the absolute value of the relative error between the results of the dual coupled RTE-DA model and the RTE based model.
  - Compared with the corresponding accuracy of the DA based model.

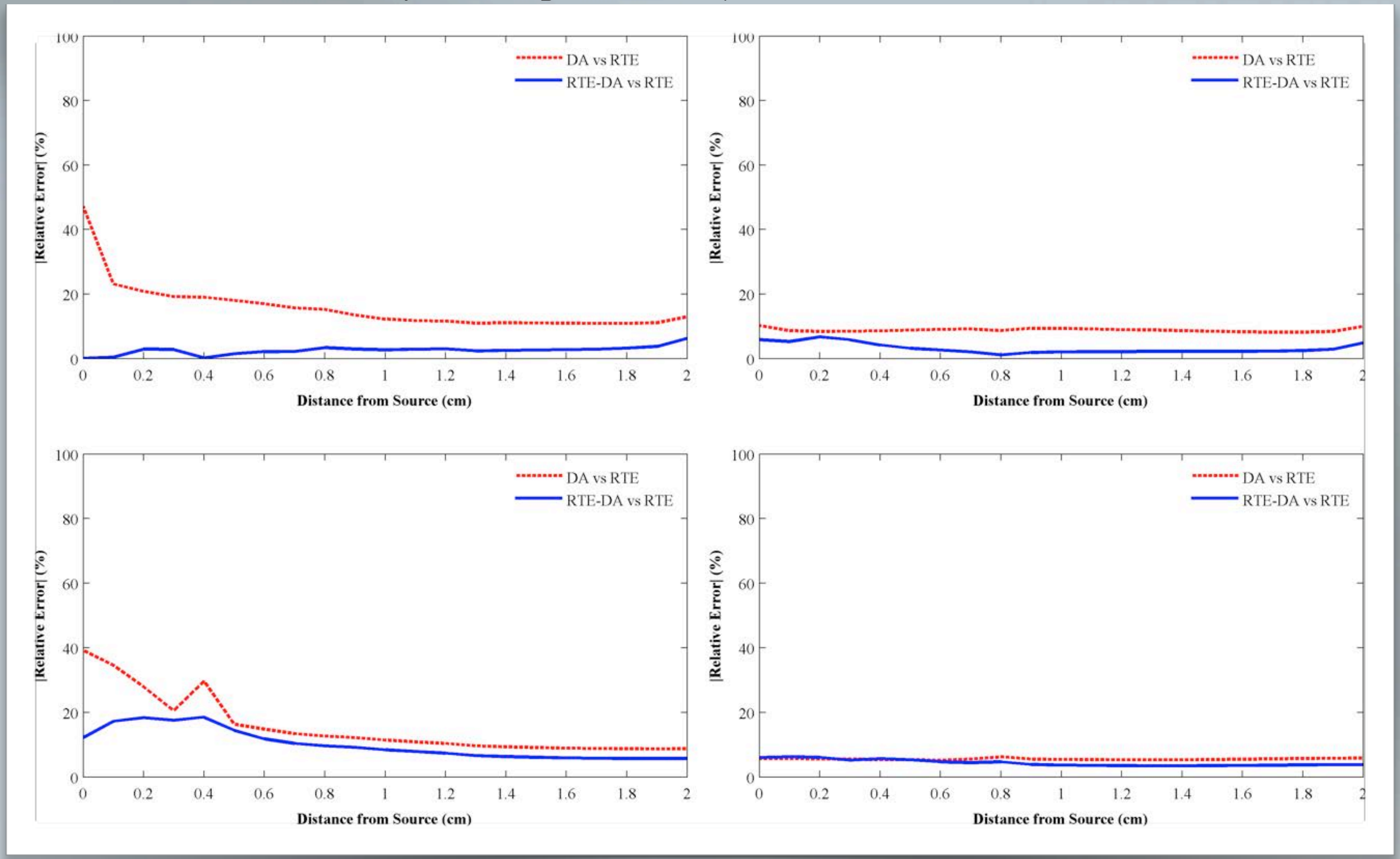

Evaluation in Frequency Domain

Evaluation of the results in the frequency domain

- Accuracy of the method.

	RTE-DA/RTE		DA/RTE	
	Excitation	Emission	Excitation	Emission
Photon density	~98%	~96%	~85%	~90%
Phase shift	~90%	~96%	~85%	~94%

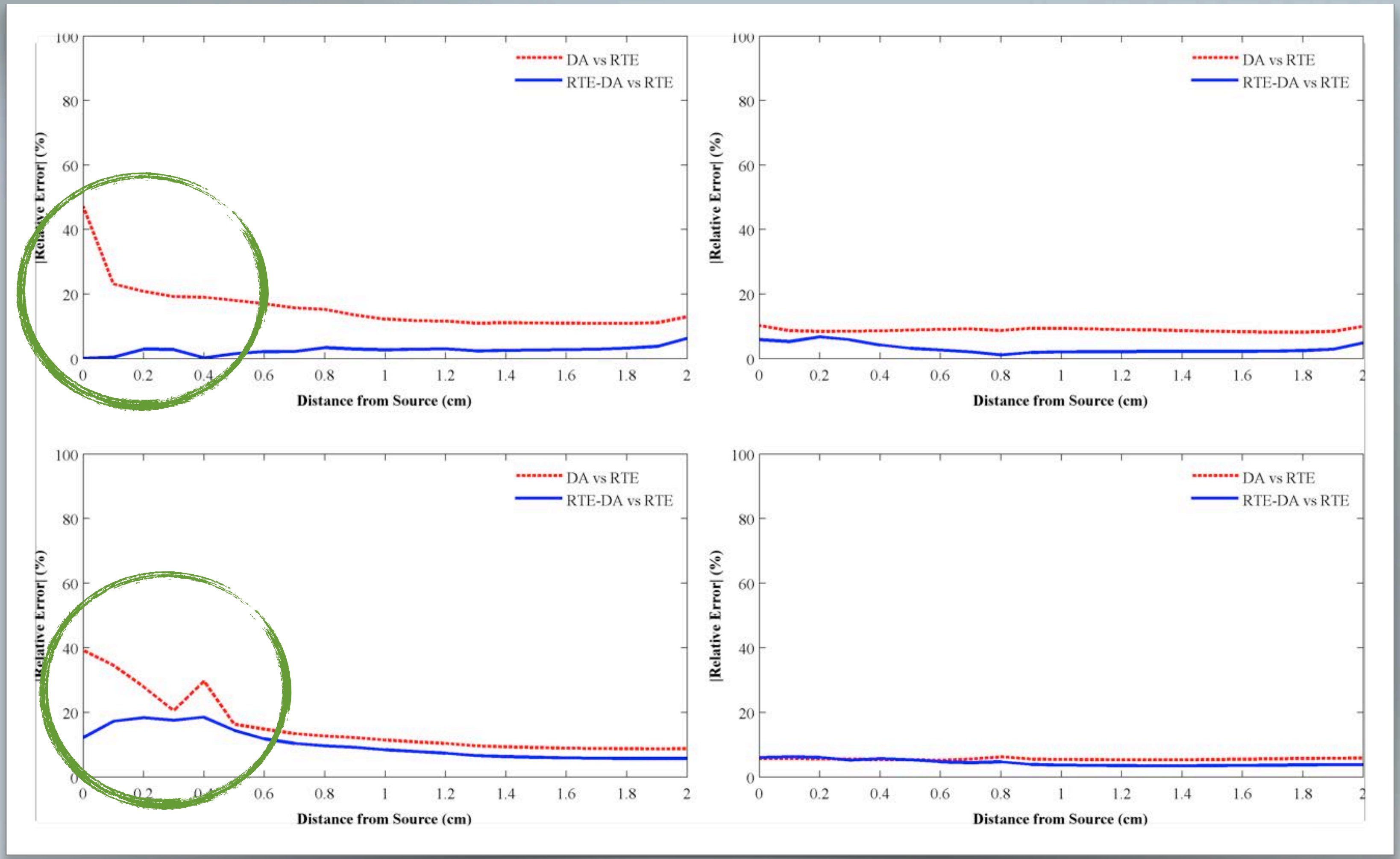

Evaluation in Frequency Domain

Evaluation of the results in the frequency domain

- The computational time, the number of iterations and the size of the formulated matrices.

	DA	RTE	RTE-DA
t_{total} (sec)	38.15	1060.19	480.74
n_x	73	101	127
n_m	76	165	197
N_{nz}	128 581	48 346 456	8 415 584
N_{total}	85 766 121	34 306 448 400	1 867 795 524

Evaluation in Frequency Domain

Evaluation of the results in the frequency domain

- The computational time, the number of iterations and the size of the formulated matrices.

	DA	RTE	RTE-DA
t_{total} (sec)	38.15	1060.19	480.74
n_x	73	101	127
n_m	76	165	197
N_{nz}	128 581	48 346 456	8 415 584
N_{total}	85 766 121	34 306 448 400	1 867 795 524

Evaluation of the Steady-State Formalism

Steady-state results

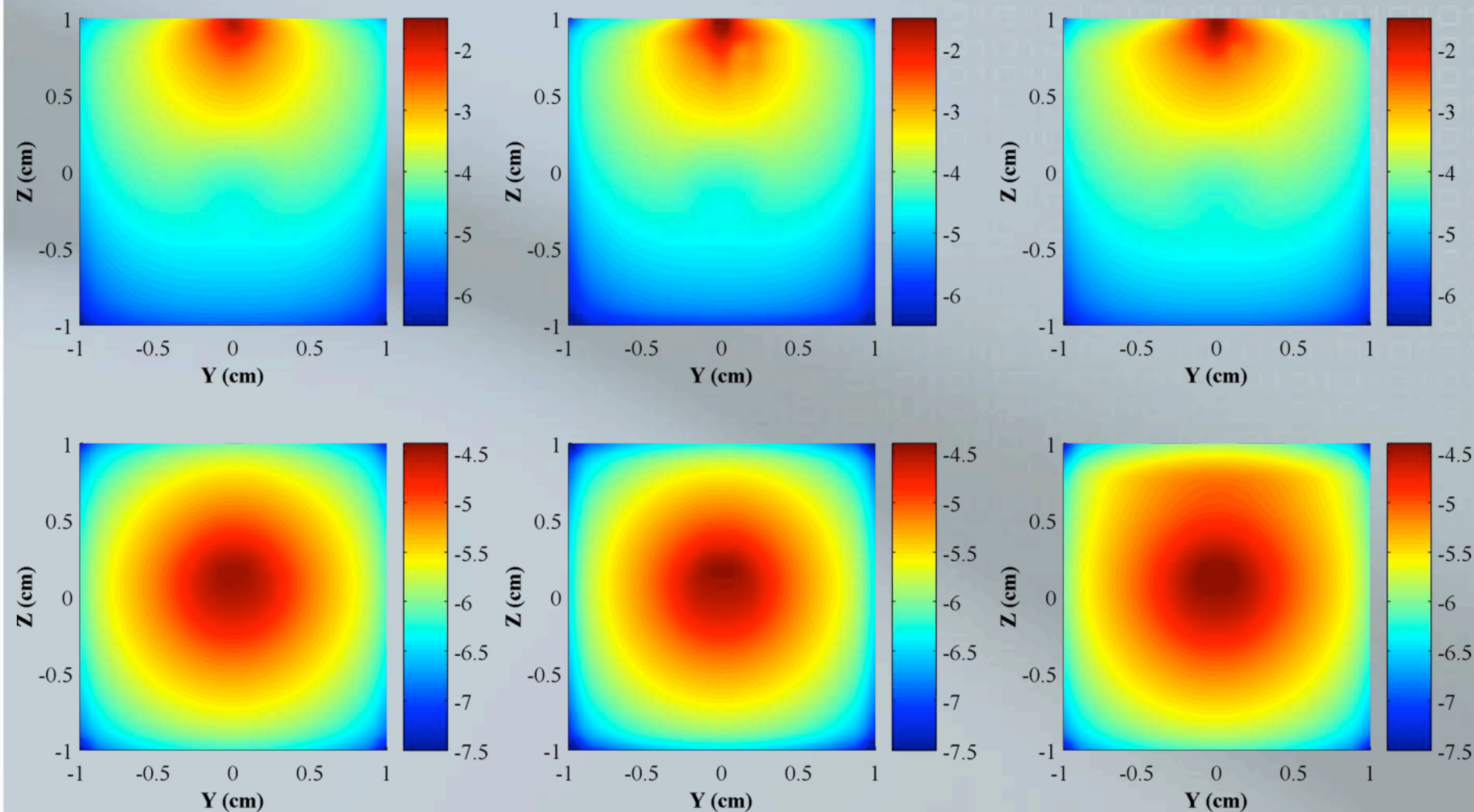

Evaluation of the Steady-State Formalism

Steady-state results

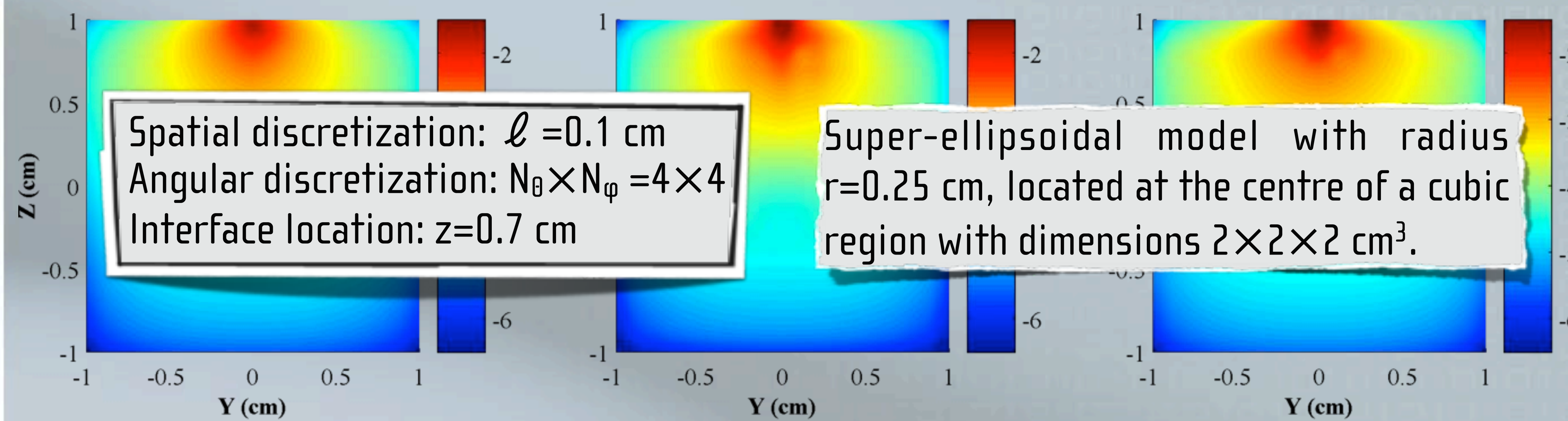

Spatial discretization: ℓ =0.1 cm
Angular discretization: $N_\theta \times N_\varphi$ =4×4
Interface location: z=0.7 cm

Super-ellipsoidal model with radius r=0.25 cm, located at the centre of a cubic region with dimensions 2×2×2 cm^3.

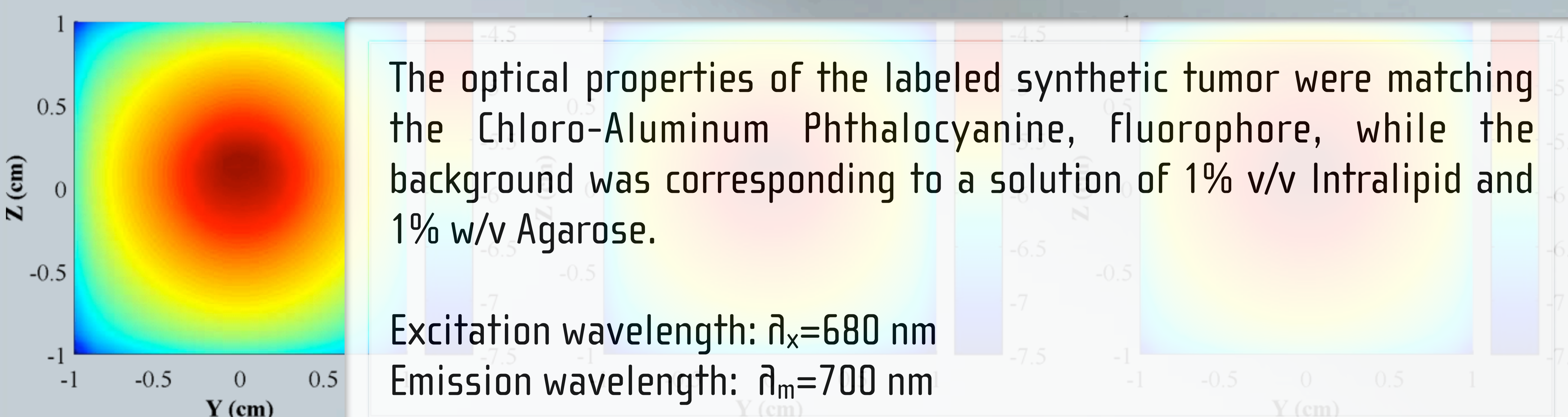

The optical properties of the labeled synthetic tumor were matching the Chloro-Aluminum Phthalocyanine, fluorophore, while the background was corresponding to a solution of 1% v/v Intralipid and 1% w/v Agarose.

Excitation wavelength: λ_x=680 nm
Emission wavelength: λ_m=700 nm

Evaluation of the Steady-State Formalism

Steady-state results

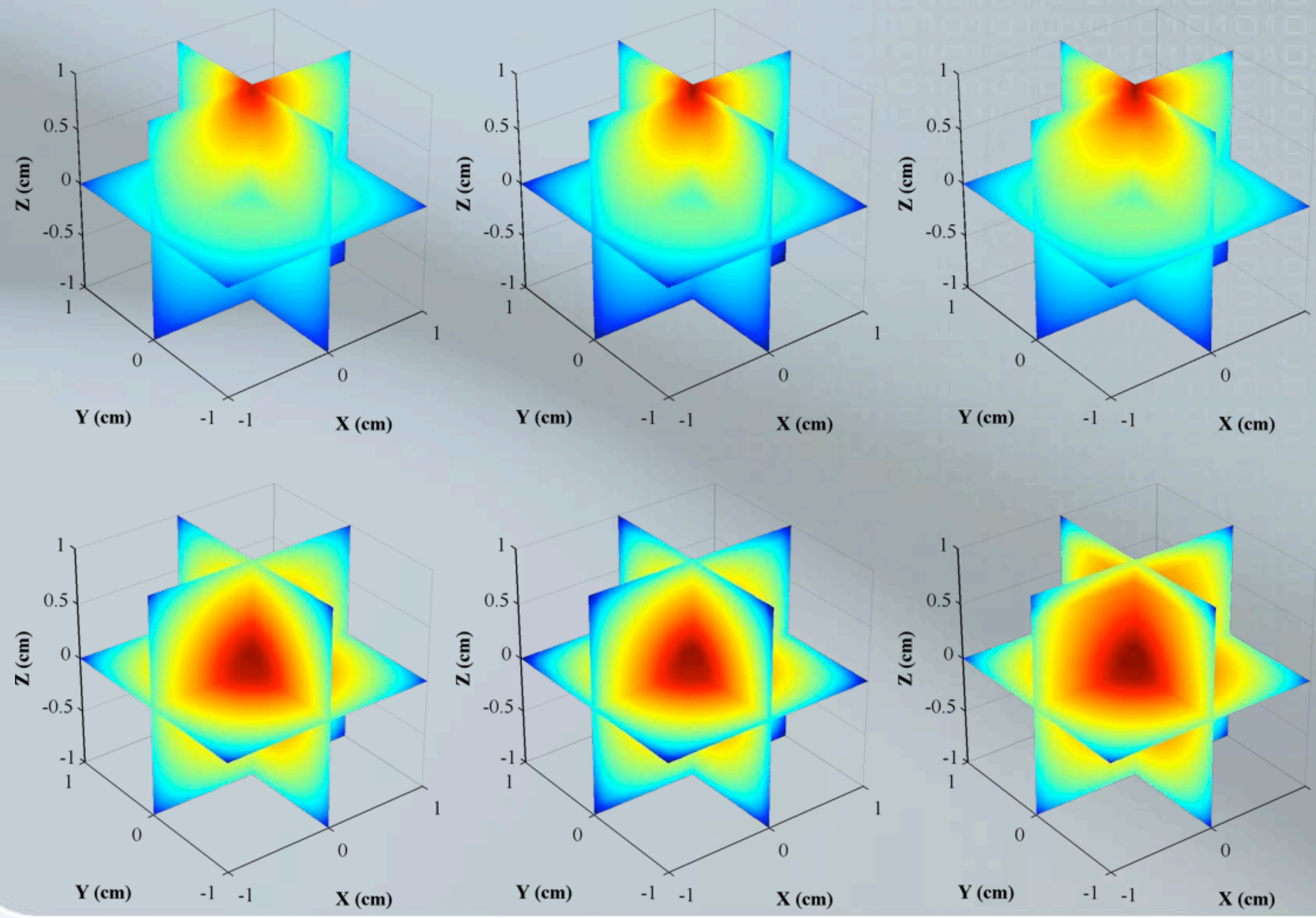

Evaluation of the Steady-State Formalism

Evaluation of the steady-state results

- Accuracy of the method.

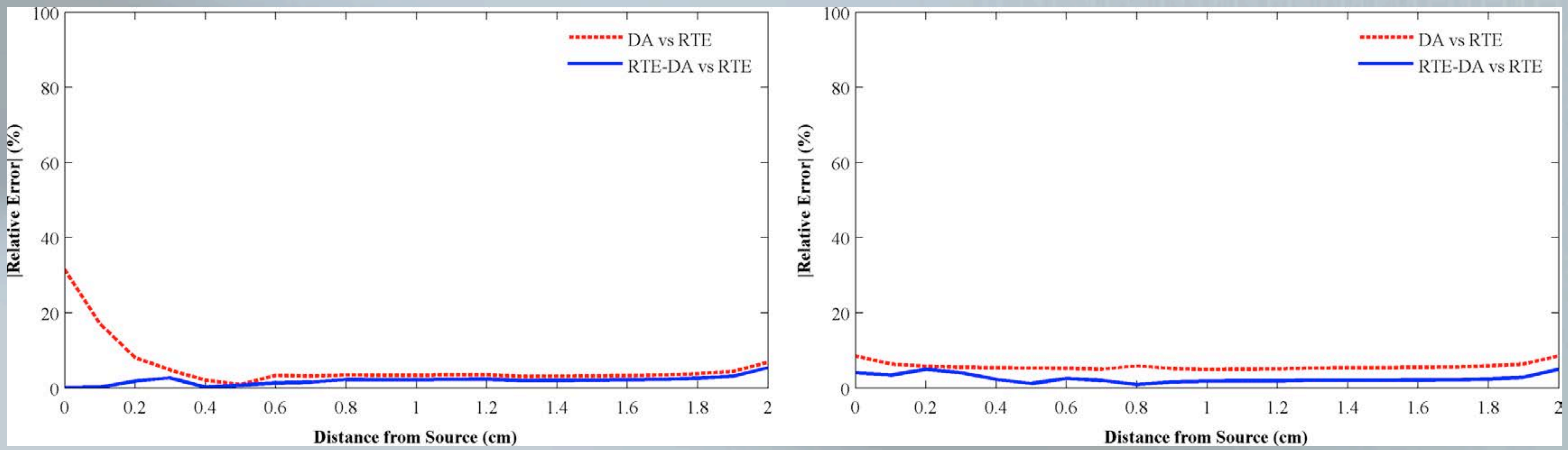

Evaluation of the Steady-State Formalism

Evaluation of the steady-state results

- Accuracy of the method.

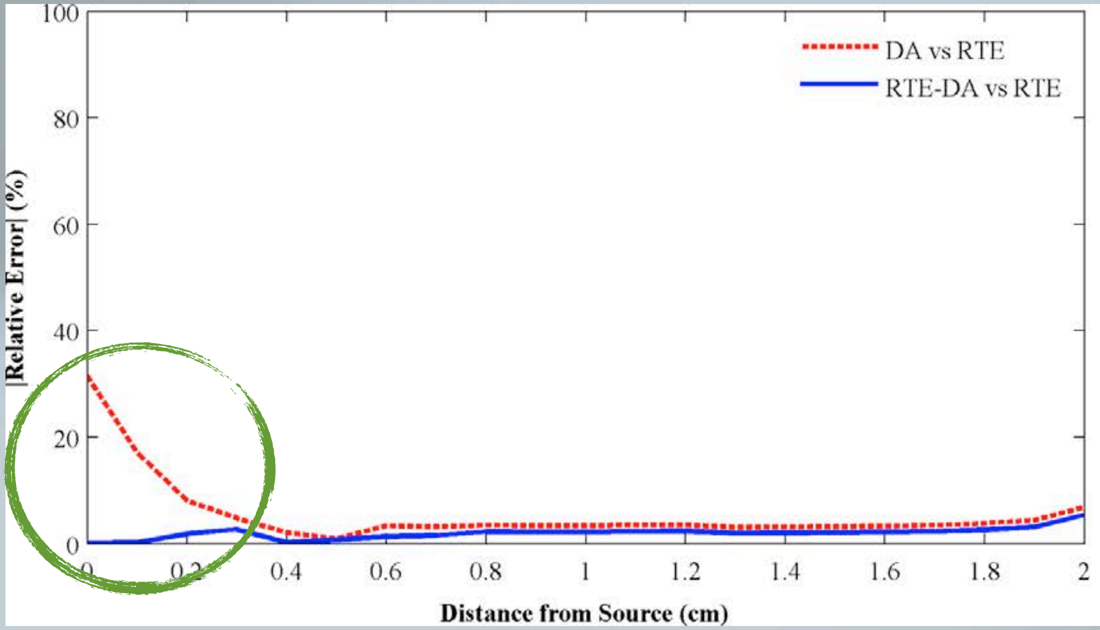

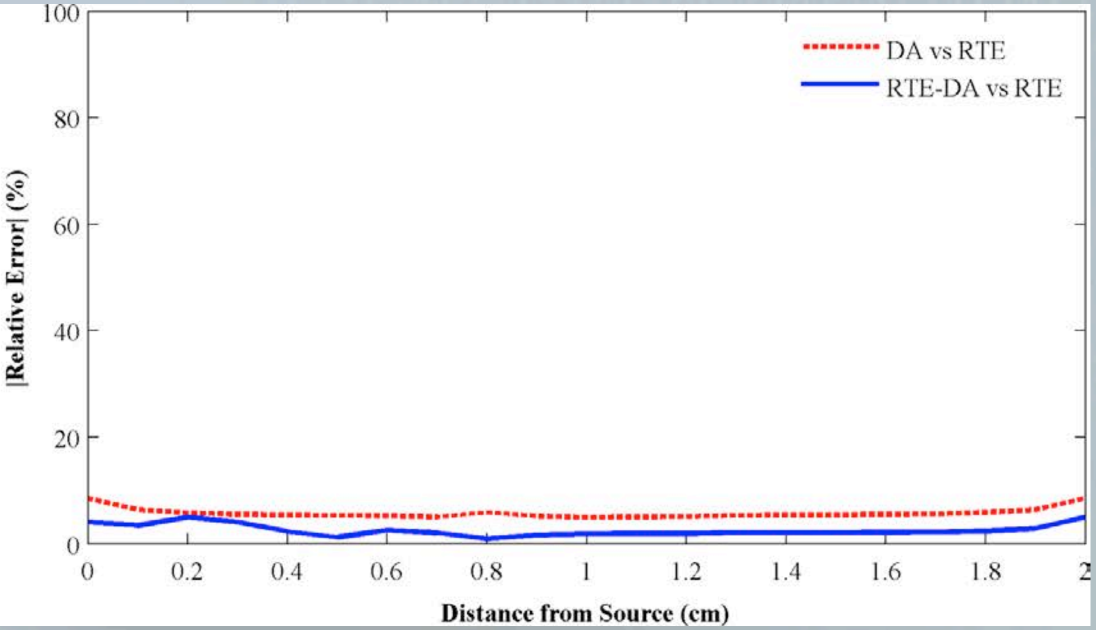

	RTE-DA/RTE		DA/RTE	
	Excitation	Emission	Excitation	Emission
Photon Density	~98%	~98%	~94%	~94%

Evaluation of the Steady-State Formalism

Evaluation of the results on the CW state

- The computational time, the number of iterations and the size of the formulated matrices.

	DA	RTE	RTE-DA
t_{total} (sec)	29.41	884.58	454.03
n_x	81	107	123
n_m	76	159	206
N_{nz}	134 864	48 346 456	8 415 584
N_{total}	94 128 804	34 306 448 400	1 867 795 524

Evaluation of the Steady-State Formalism

Evaluation of the results on the CW state

- The computational time, the number of iterations and the size of the formulated matrices.

	DA	RTE	RTE-DA
t_{total} (sec)	29.41	884.58	454.03
n_x	81	107	123
n_m	76	159	206
N_{nz}	134 864	48 346 456	8 415 584
N_{total}	94 128 804	34 306 448 400	1 867 795 524

Evaluation with Real Measurements

Construction of the database

- Solution of the forward problem for numerous virtual fluorophores distributions and for every excitation source position.

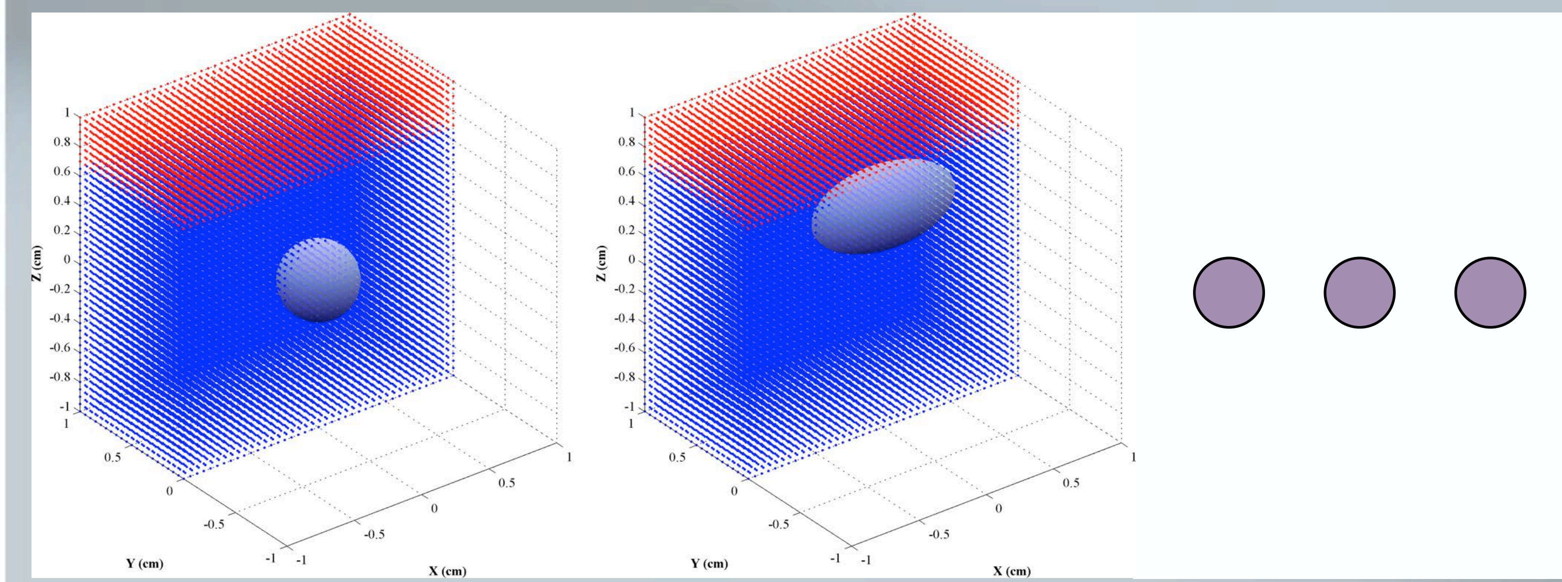

Dual coupled RTE-DA model

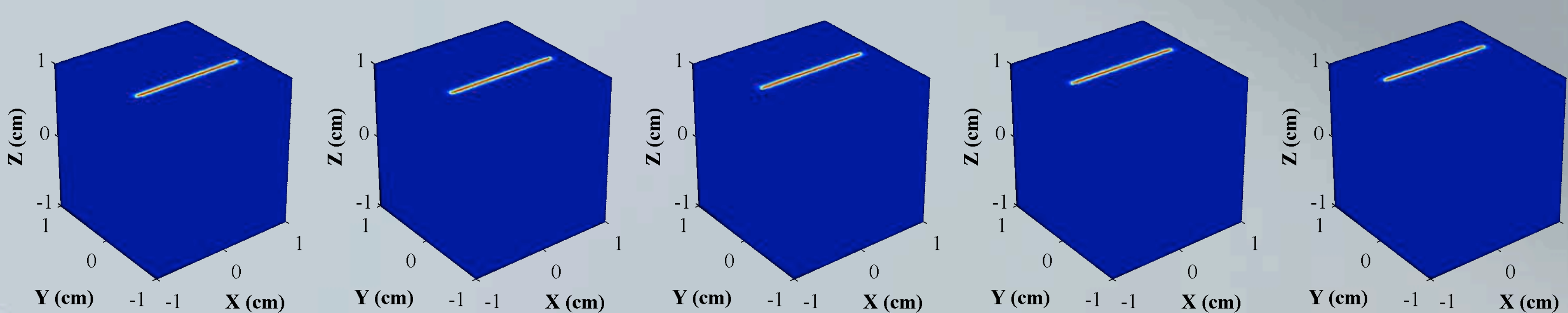

Evaluation with Real Measurements

An example of measured data

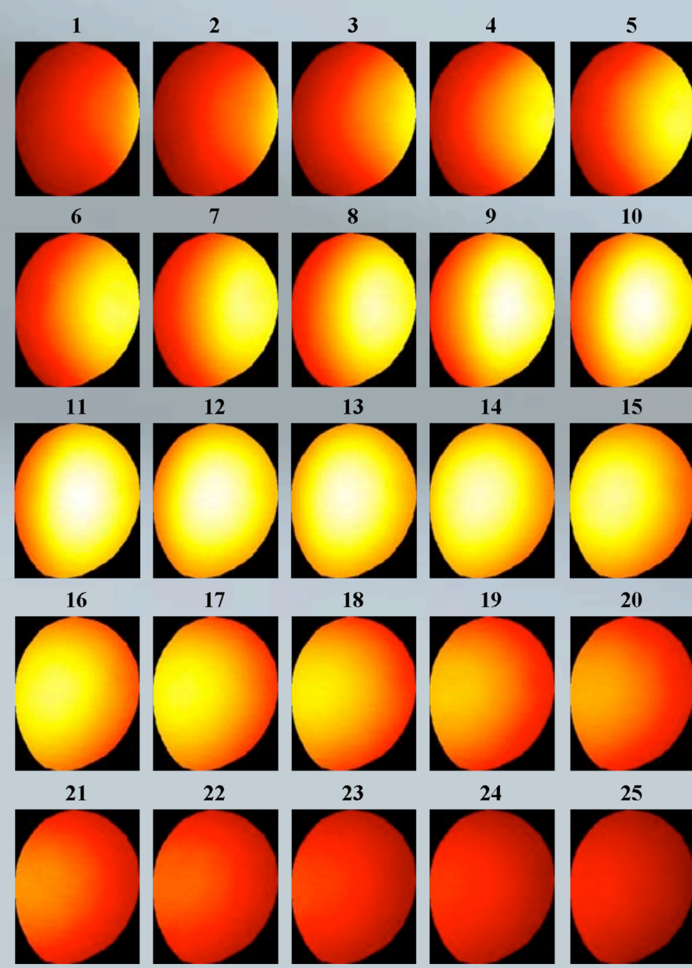

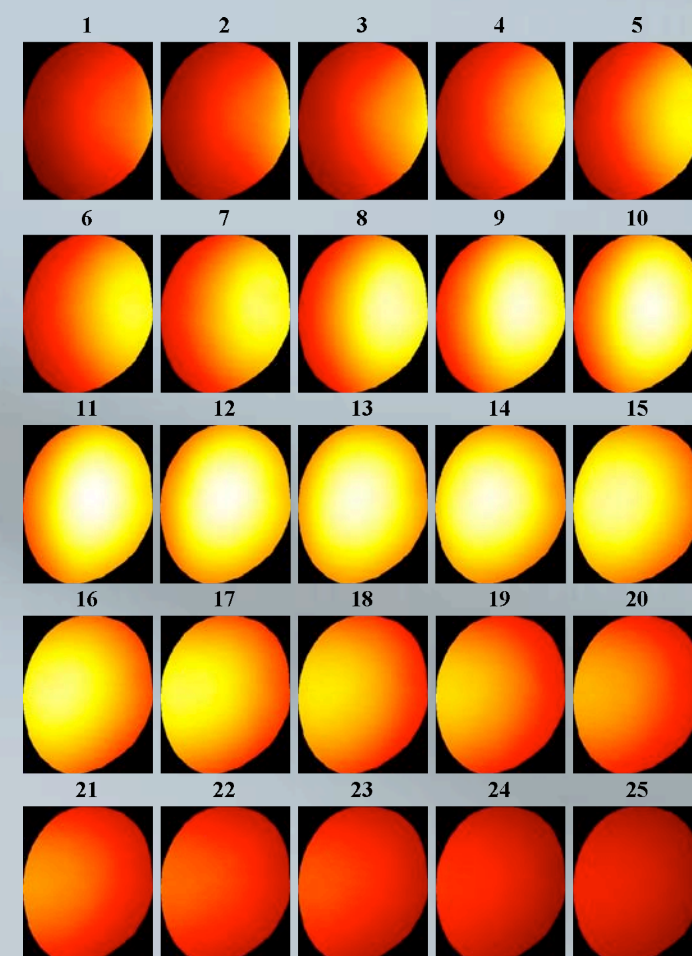

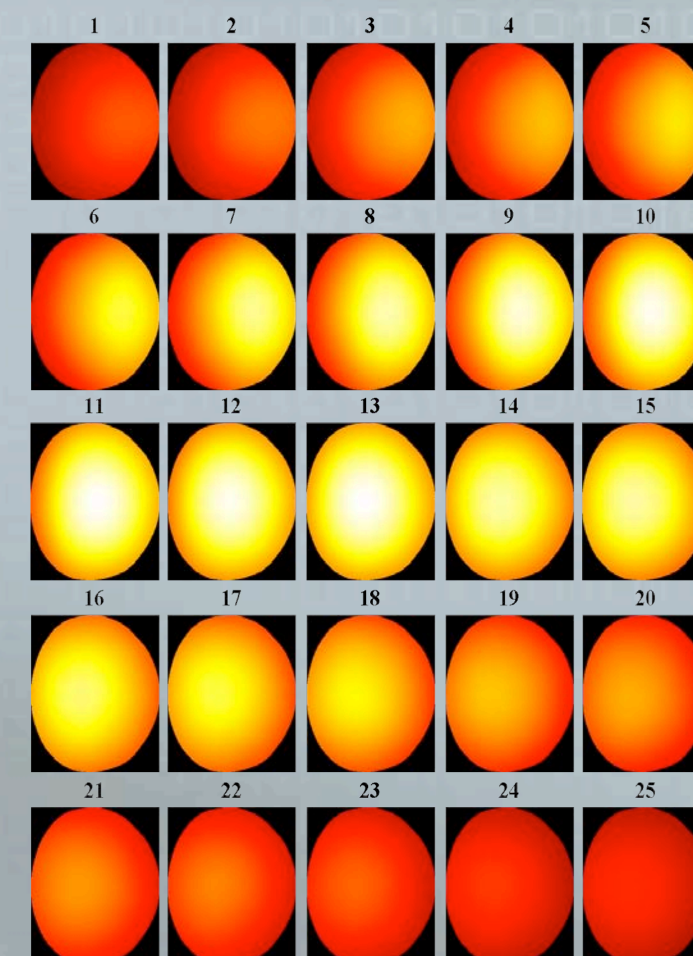

Fluorophore: Alexa Fluor 680.
Real geometry: Ellipsoidal with d=0.25cm and h=0.5cm at z=0.6cm
Tissue phantom: Suspension of 1% v/v Intralipid and 1% w/v Agarose.
Excitation source: Projected line with scanning step 0.05 cm.

Evaluation with Real Measurements

The system

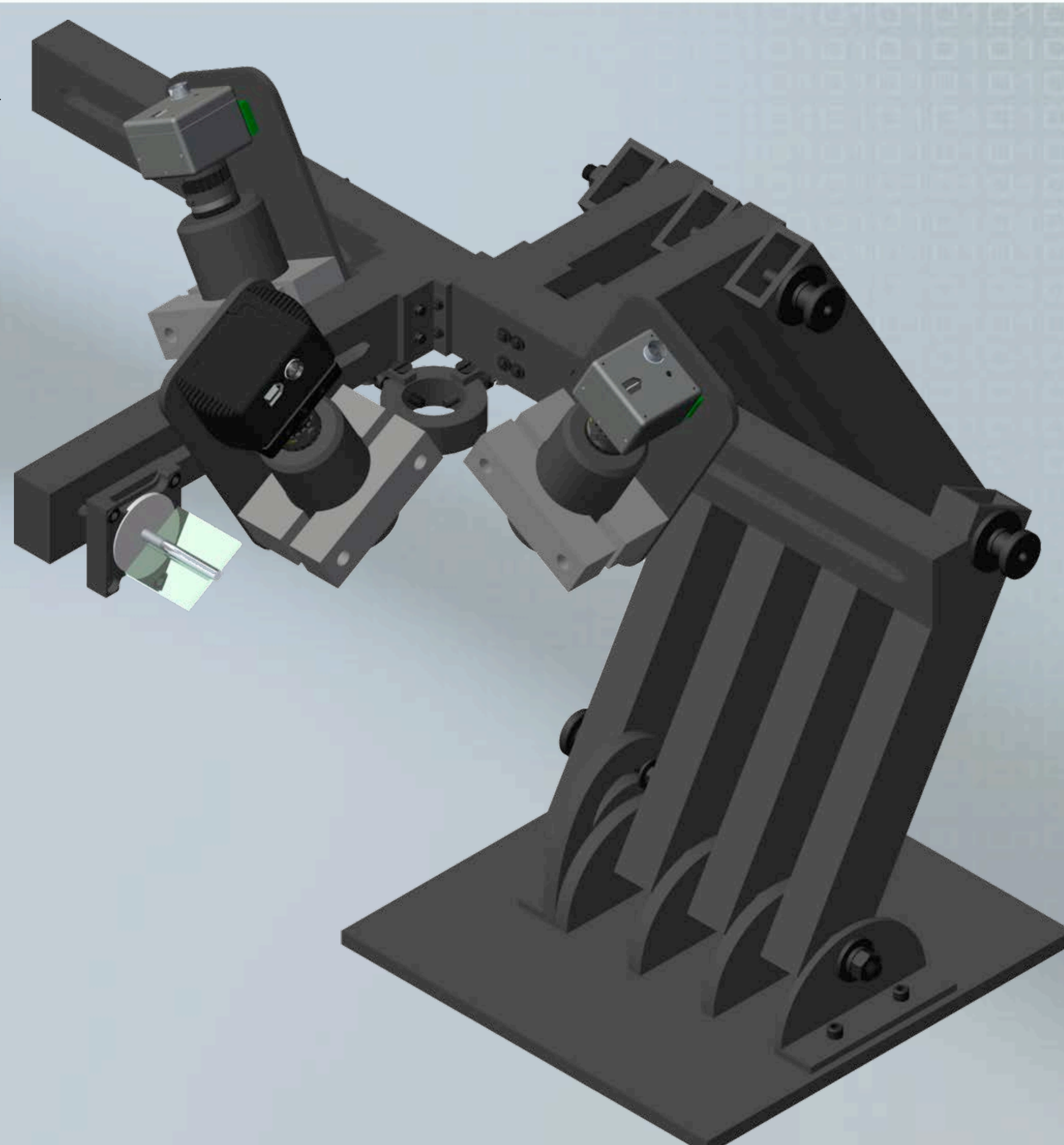

Evaluation with Real Measurements

The system

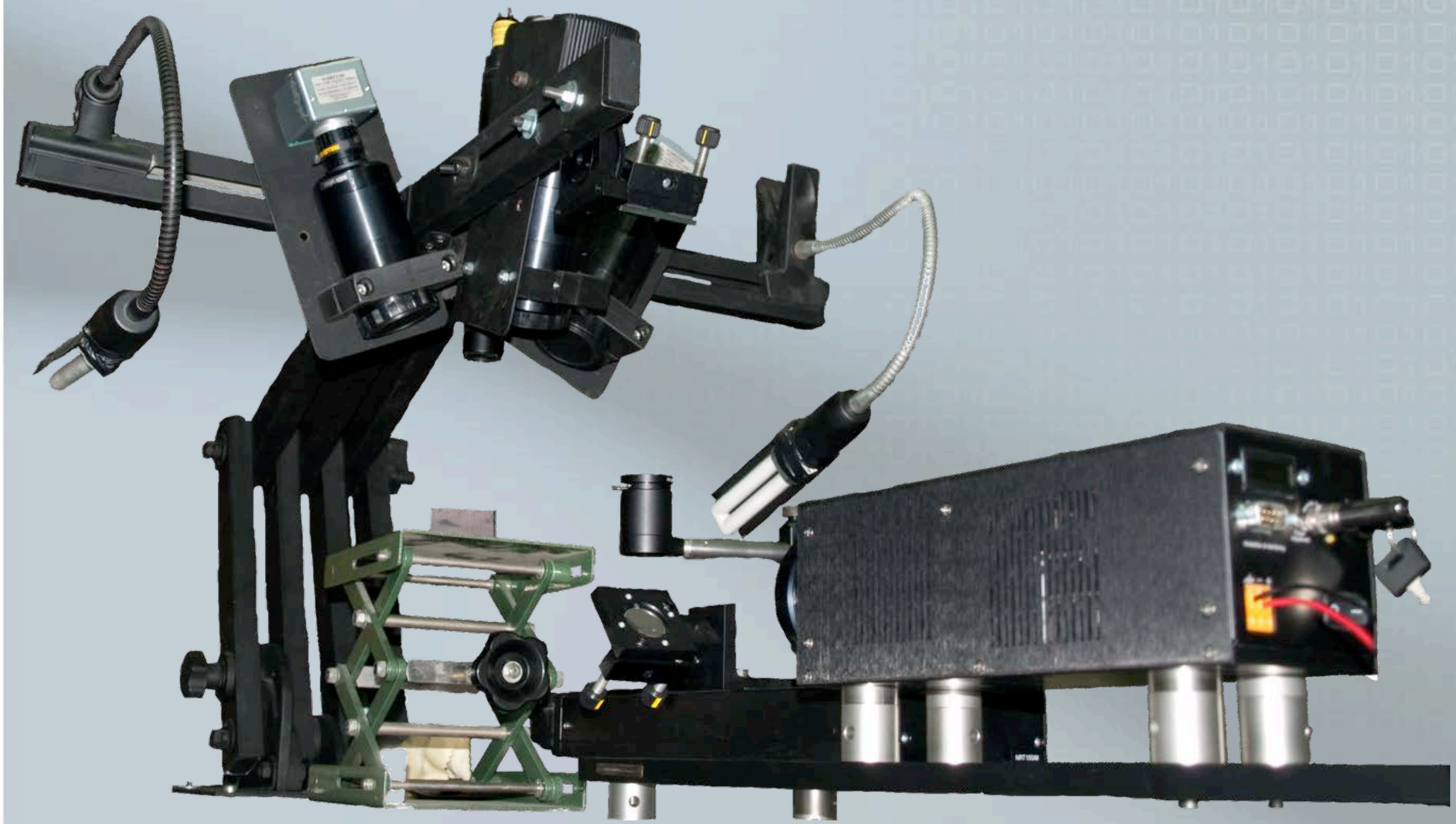

Evaluation with Real Measurements

The system

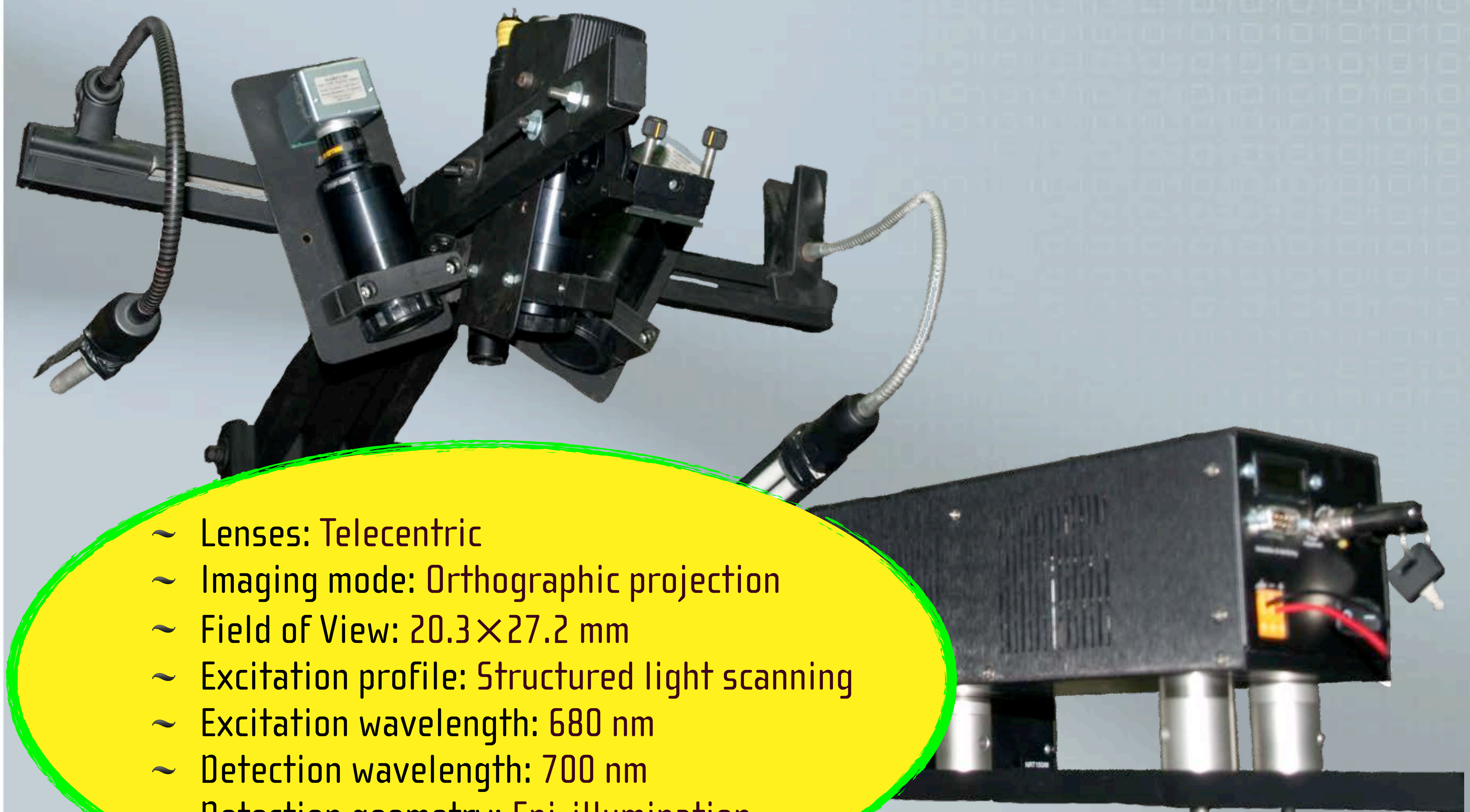

- Lenses: Telecentric
- Imaging mode: Orthographic projection
- Field of View: 20.3×27.2 mm
- Excitation profile: Structured light scanning
- Excitation wavelength: 680 nm
- Detection wavelength: 700 nm
- Detection geometry: Epi-illumination

Evaluation with Real Measurements

The system

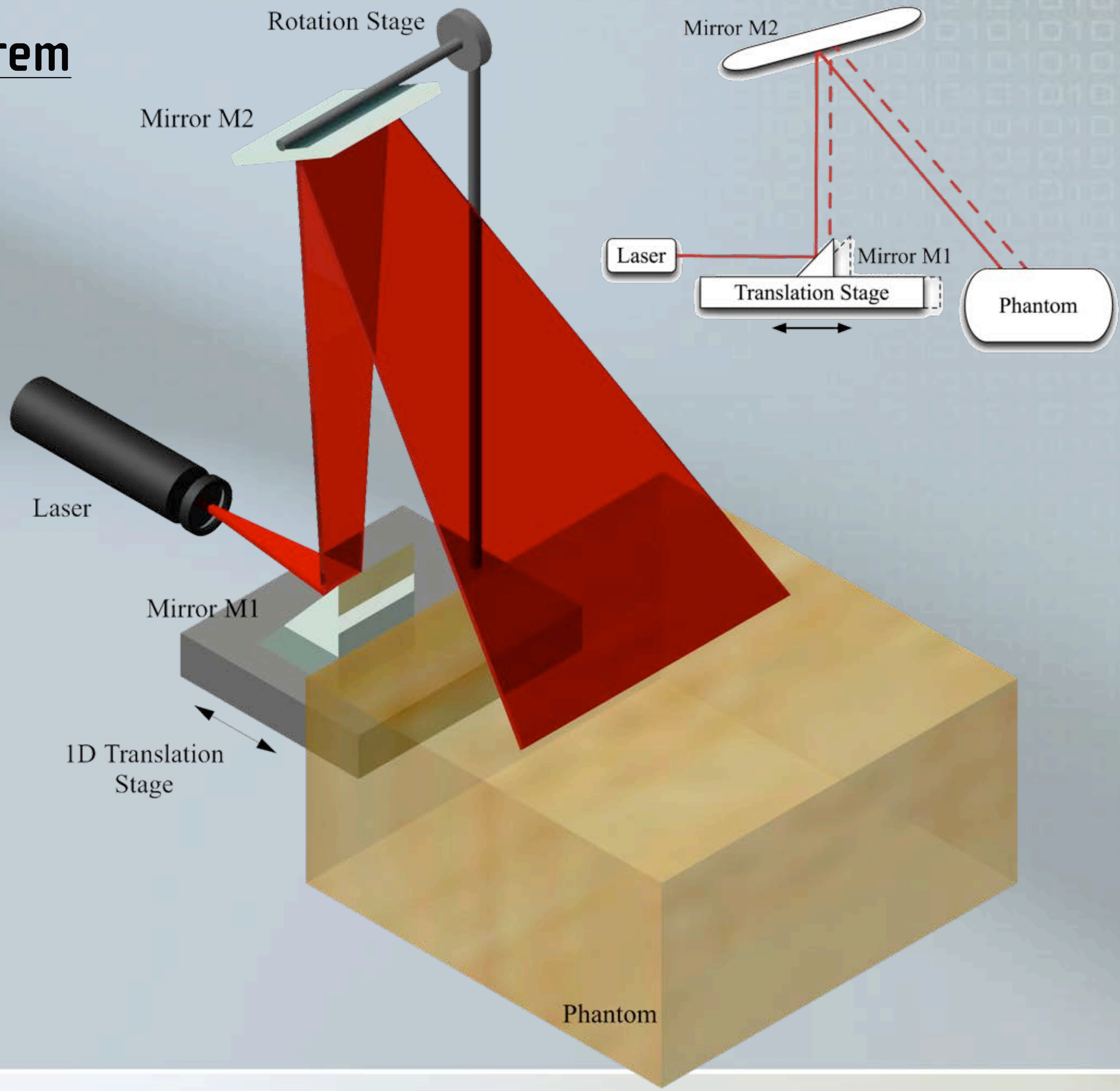

Evaluation with Real Measurements

The corresponding virtual distribution

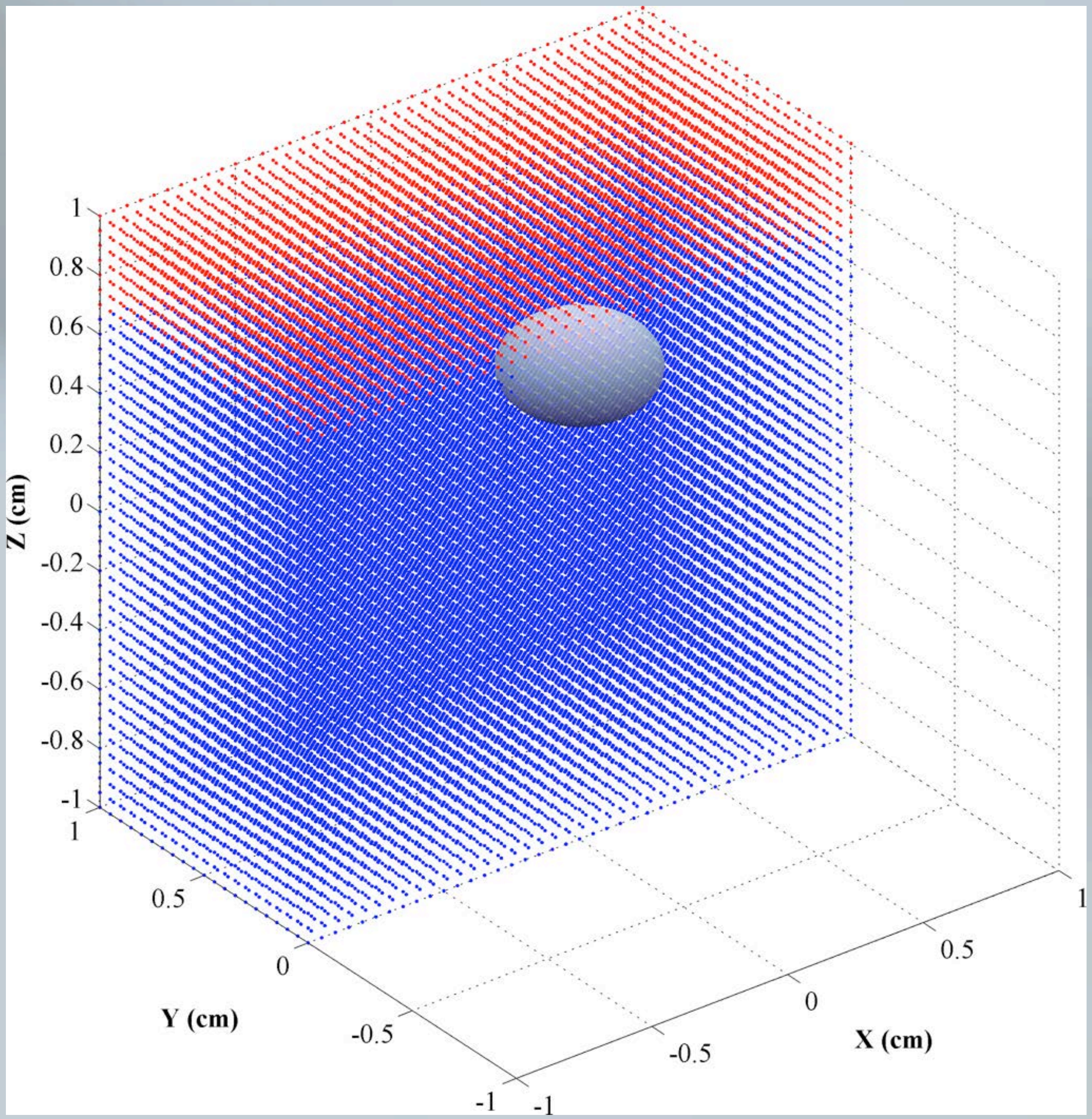

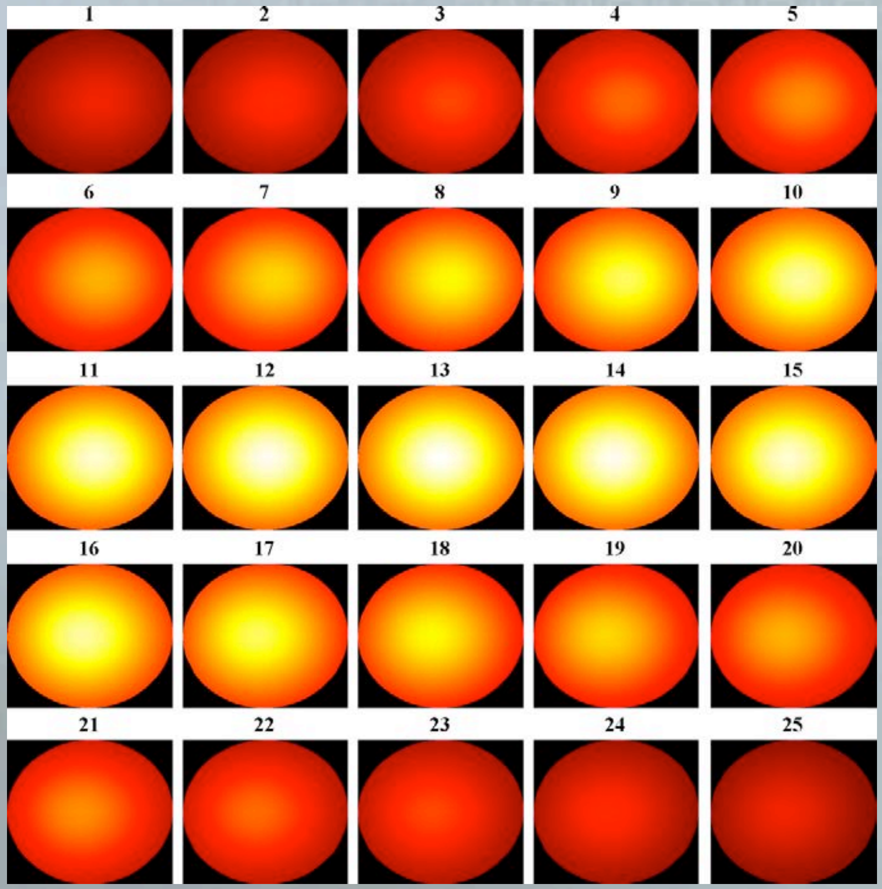

- The mean accuracy level of the correspondence between real and virtual data exceeds 80%.

Evaluation with Virtual Tissue-Like Measurements

Evaluation with application on the MOBY phantom

The various organs of this digital mouse phantom have been developed through the utilization of non-uniform rational b-spline (NURBS) surfaces. High-resolution 3D magnetic resonance microscopy (MRM) data, obtained from the Duke Center for In Vivo Microscopy, was used as the basis for the formation of the surfaces. This digital phantom has been utilized for numerous imaging studies, including fluorescence molecular imaging studies.

Evaluation with Virtual Tissue-Like Measurements

Evaluation with application on the MOBY phantom

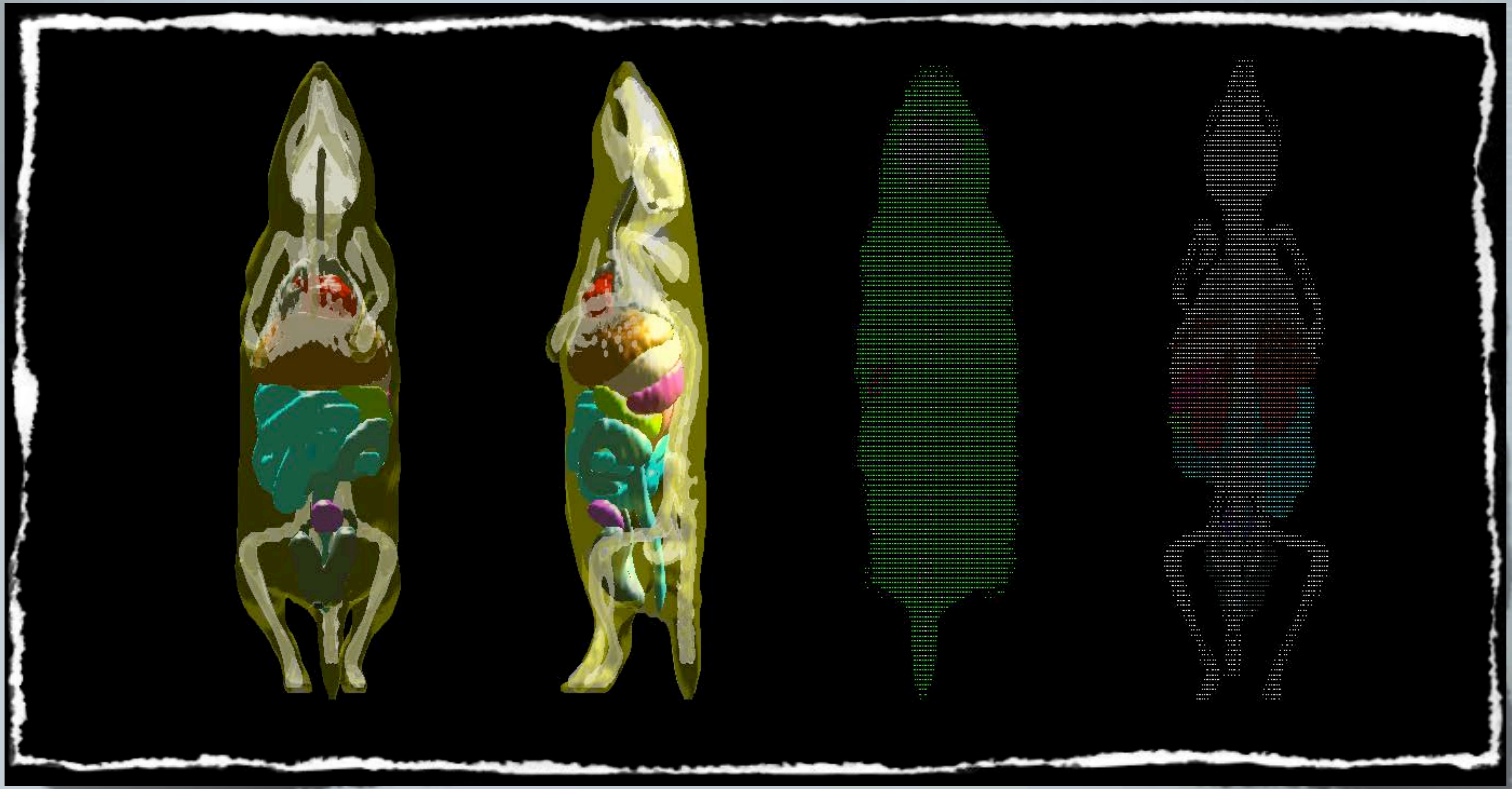

Evaluation with Virtual Tissue-Like Measurements

Evaluation with application on the MOBY phantom

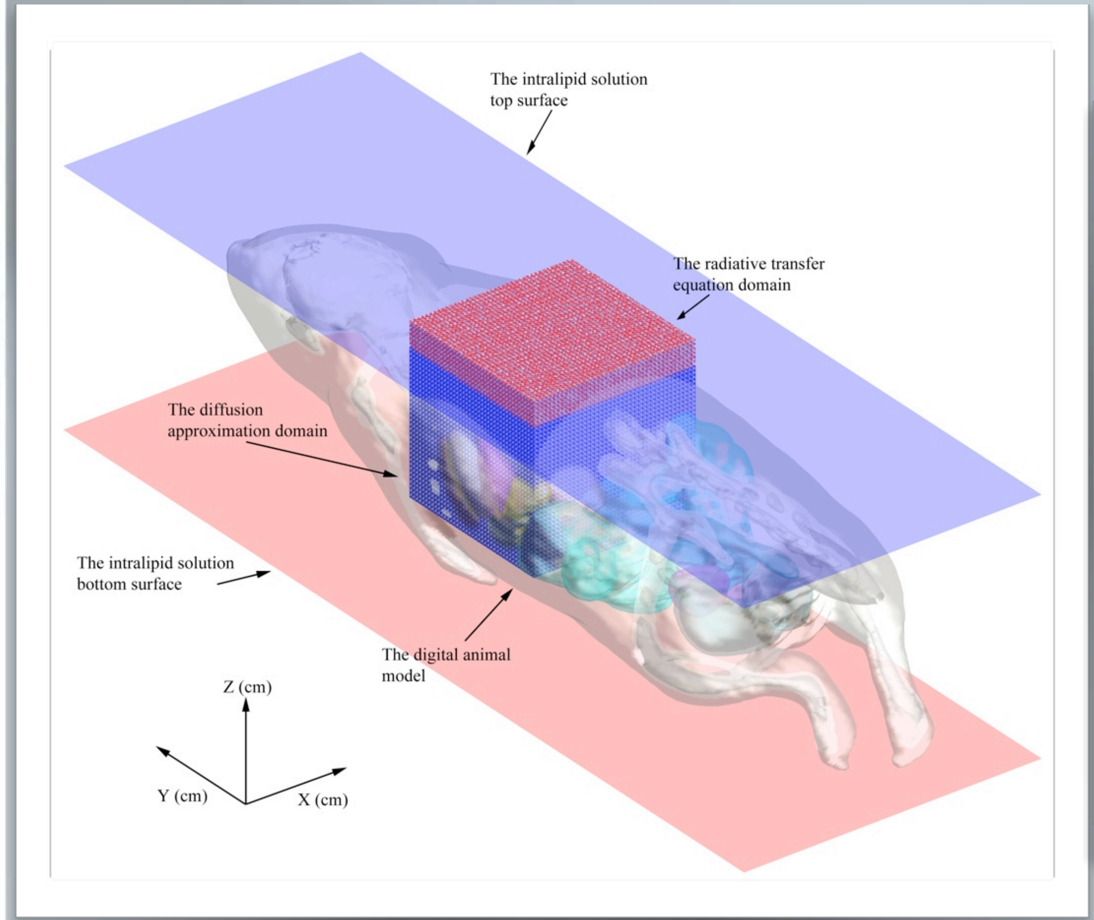

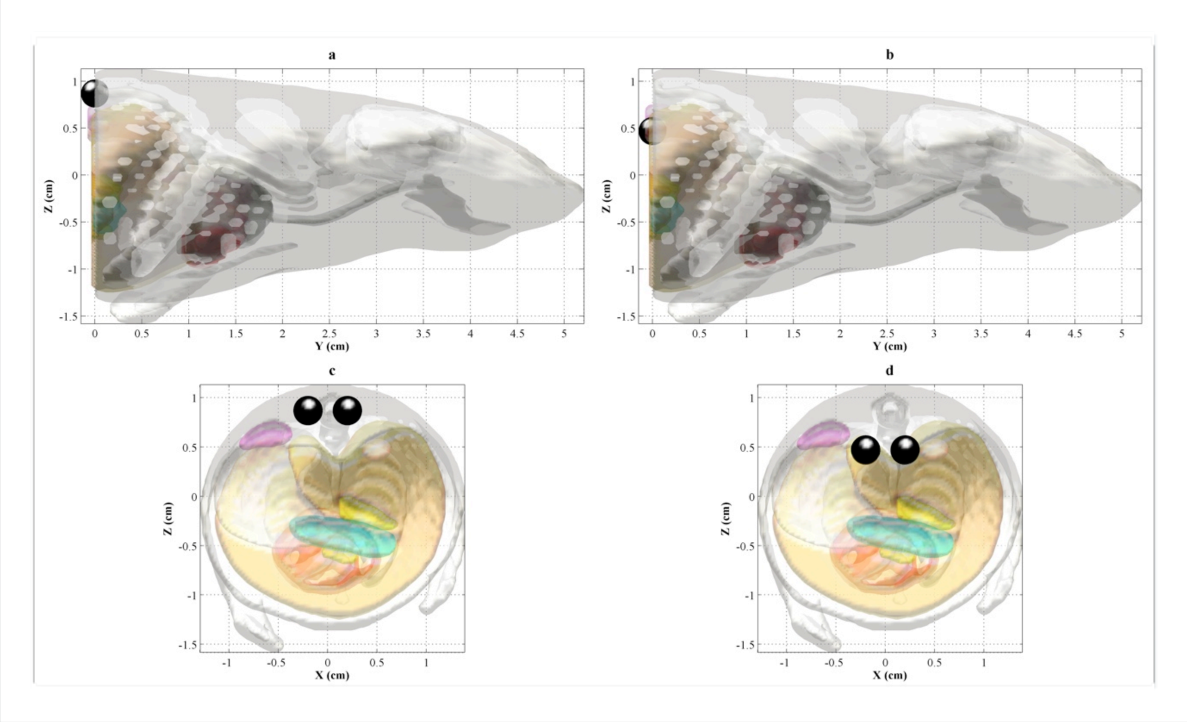

Gorpas D., and Andersson-Engels S., "Dual Coupled Radiative Transfer Equation and Diffusion Approximation for the Solution of the Forward Problem in Fluorescence Molecular Imaging", Imaging, Manipulation, and Analysis of Biomolecules, Cells, and Tissues X, Proc. SPIE, 8225:822522 (2012).

Evaluation with Virtual Tissue-Like Measurements

Evaluation with application on the MOBY phantom

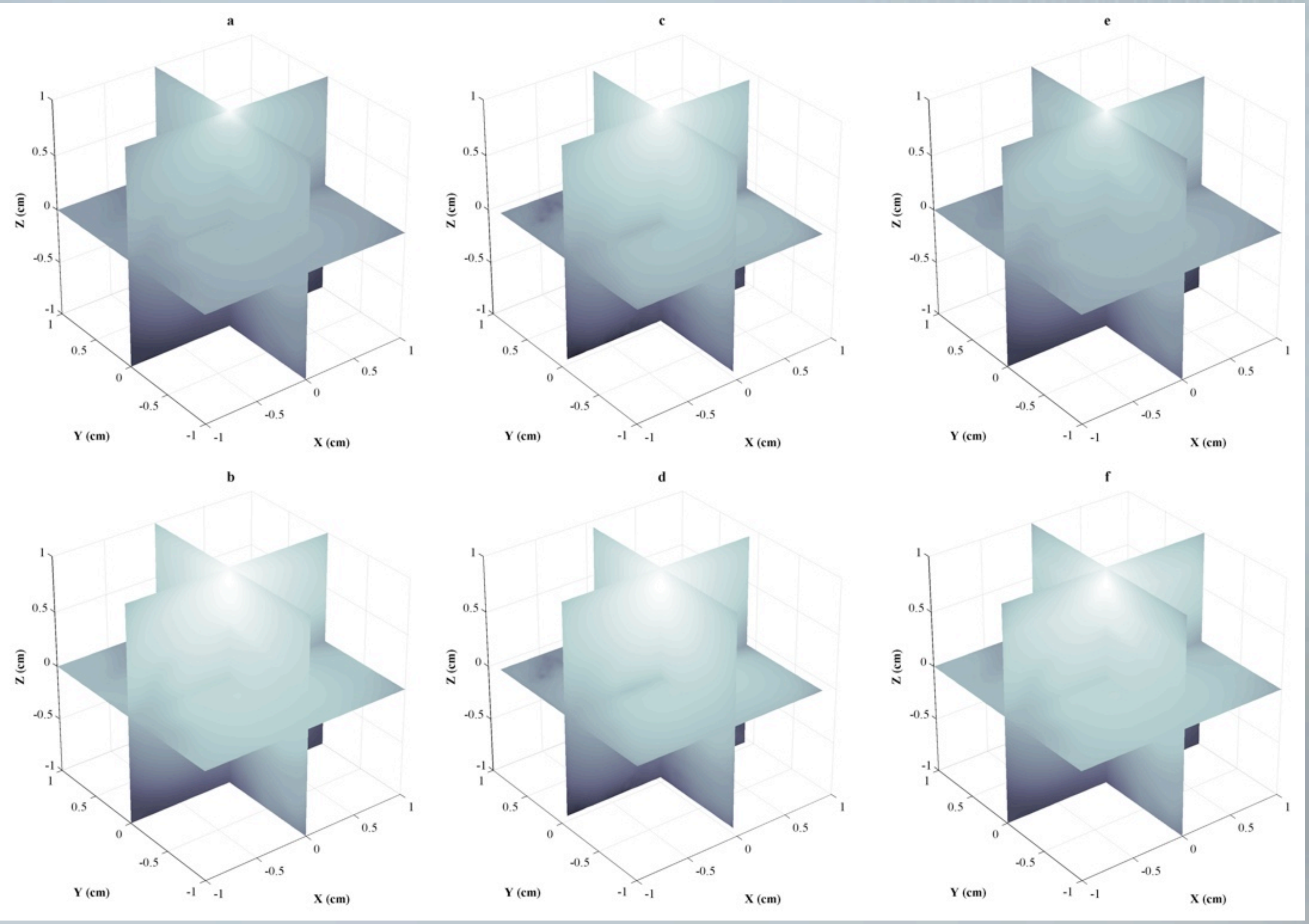

Evaluation with Virtual Tissue-Like Measurements

Evaluation with application on the MOBY phantom

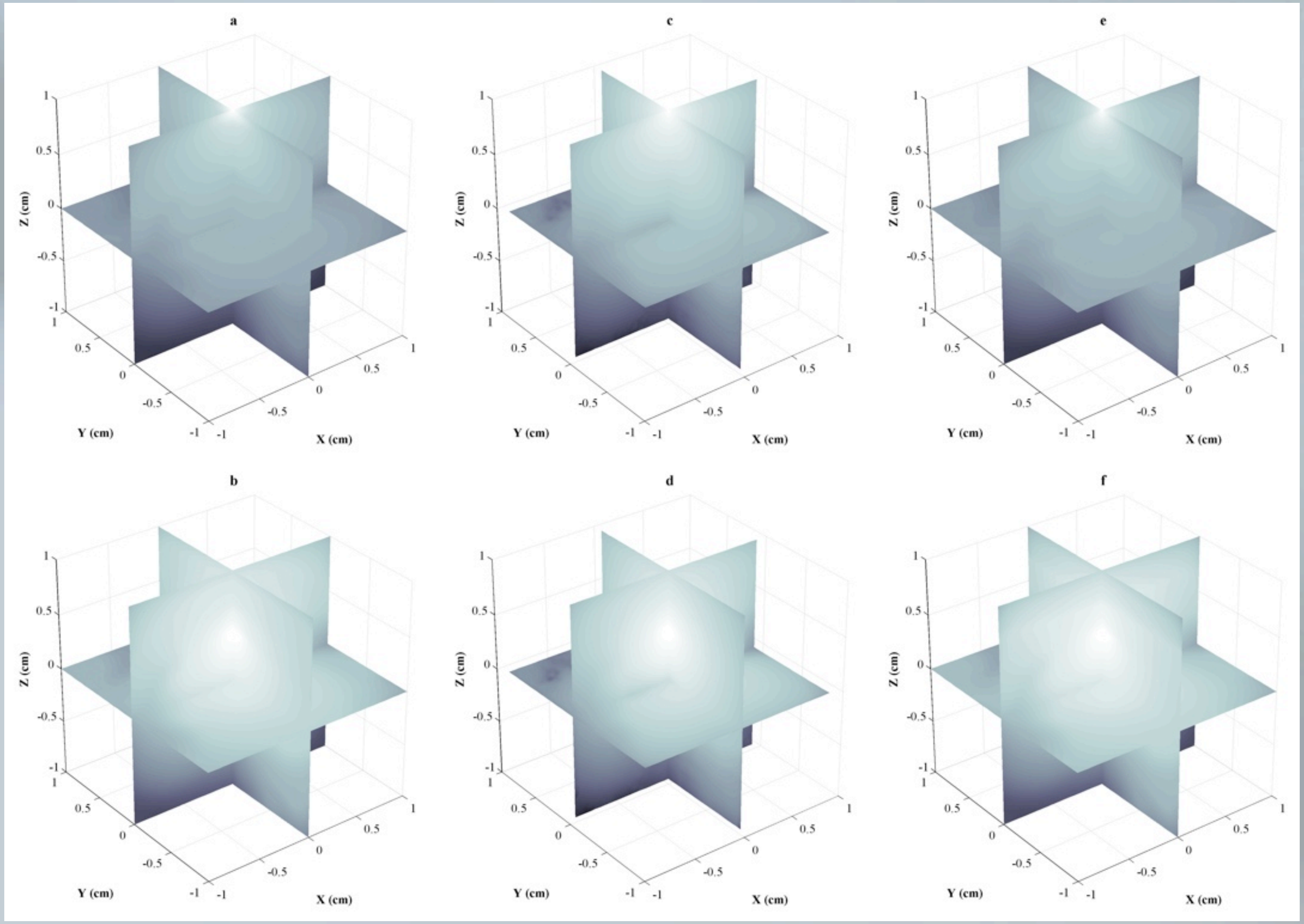

Evaluation with Virtual Tissue-Like Measurements

Evaluation with application on the MOBY phantom

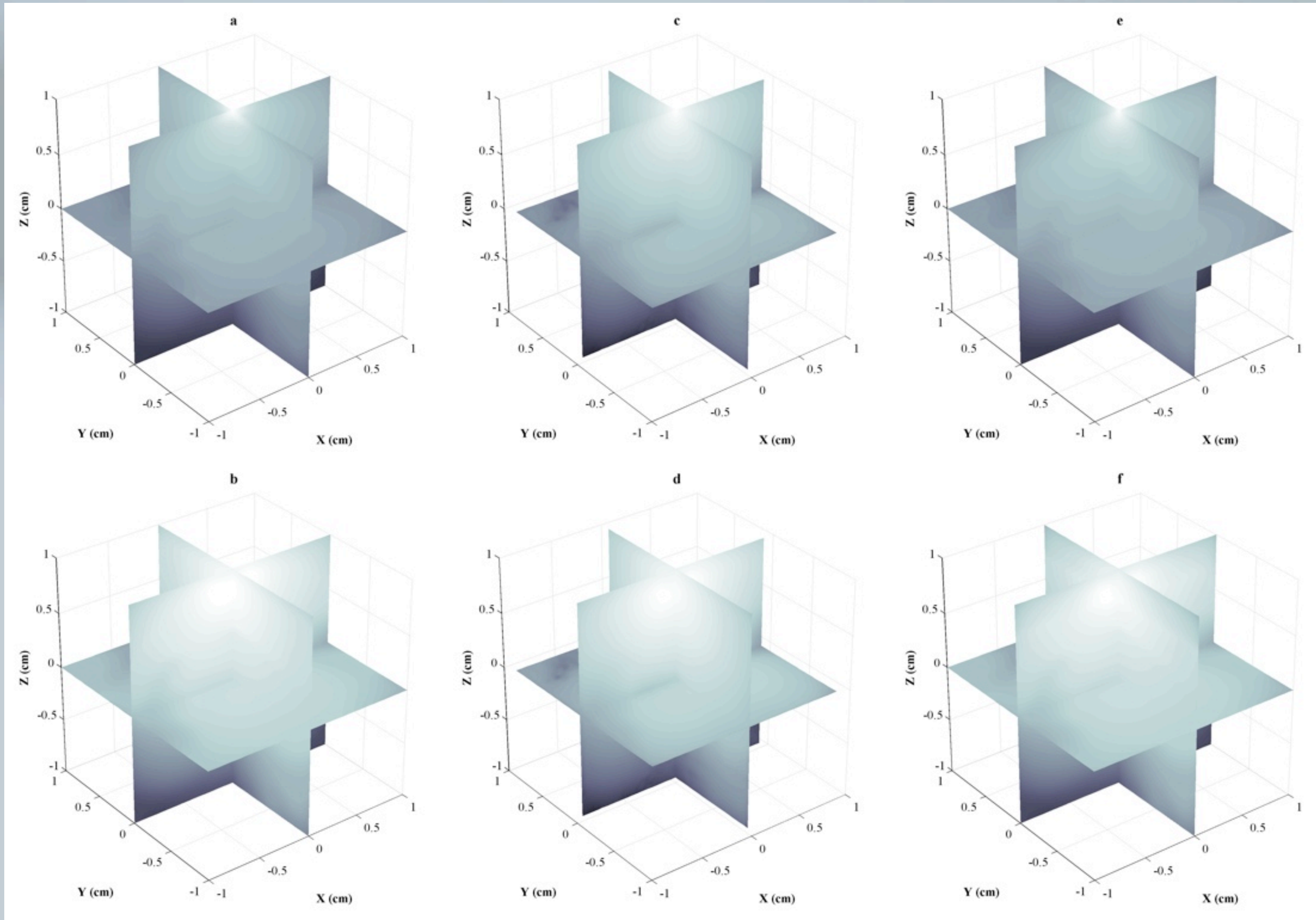

Evaluation with Virtual Tissue-Like Measurements

Evaluation with application on the MOBY phantom

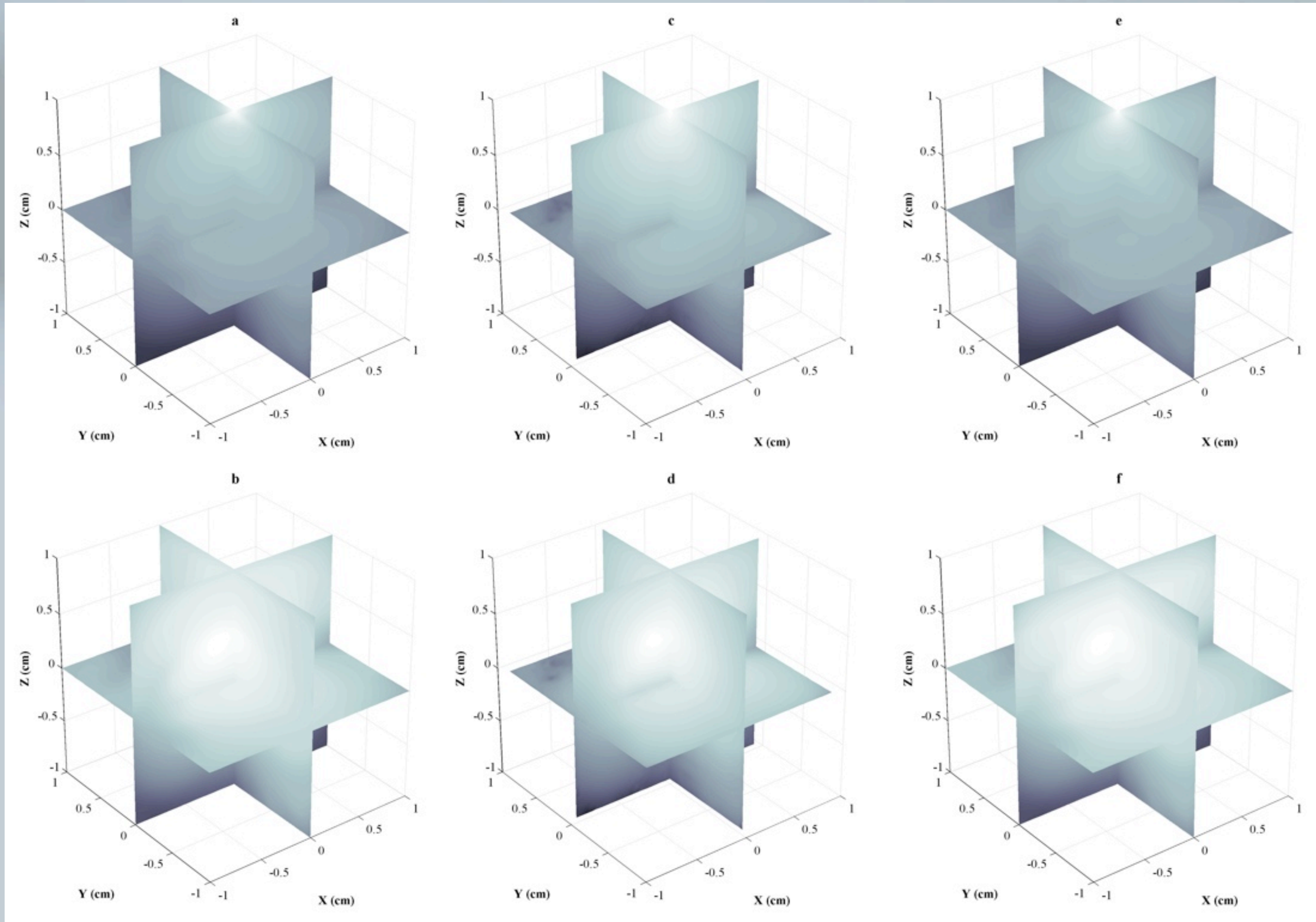

Evaluation with Virtual Tissue-Like Measurements

Evaluation with application on the MOBY phantom

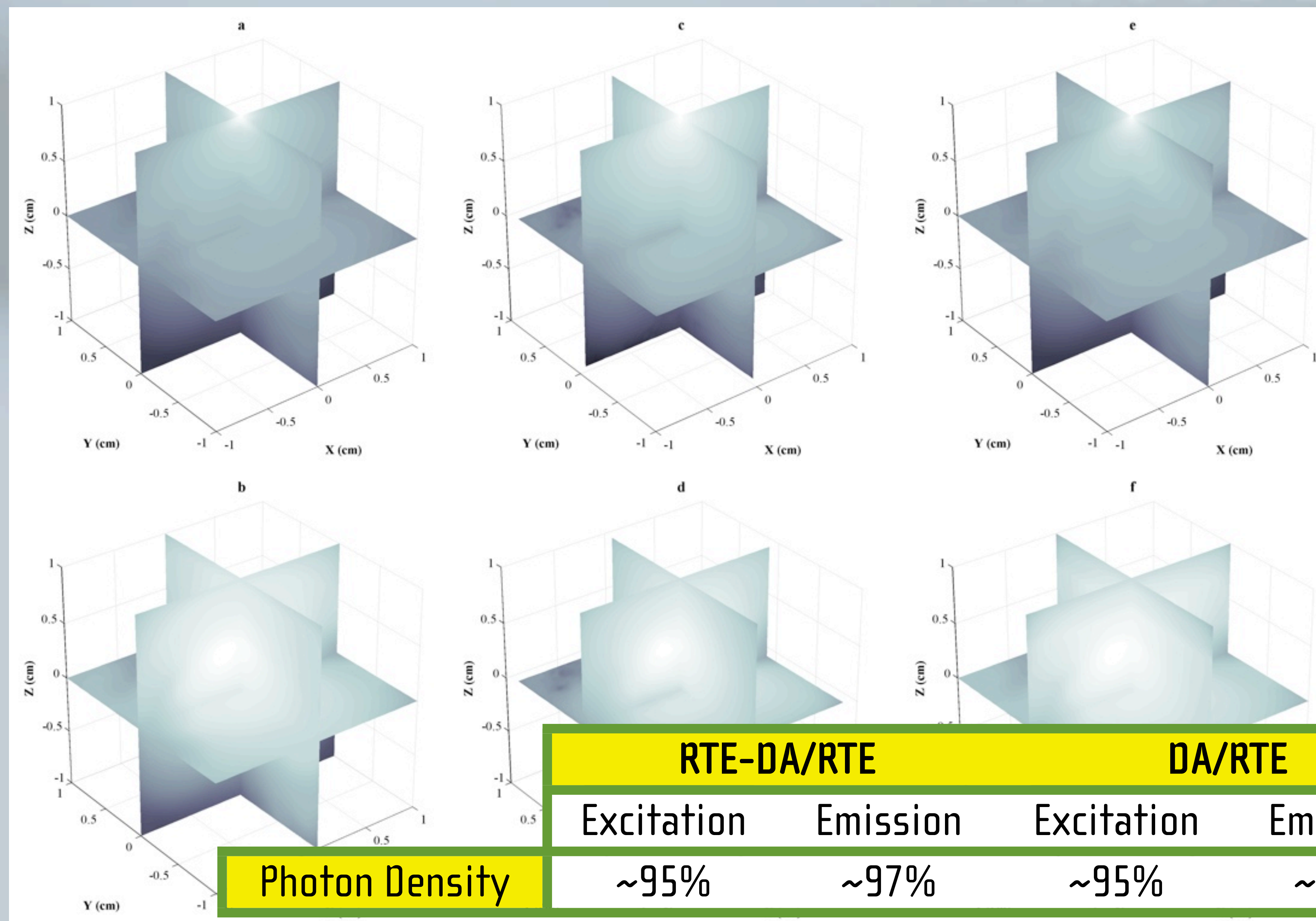

	RTE-DA/RTE		DA/RTE	
	Excitation	Emission	Excitation	Emission
Photon Density	~95%	~97%	~95%	~85%

Evaluation with Virtual Tissue-Like Measurements

Evaluation with application on the MOBY phantom

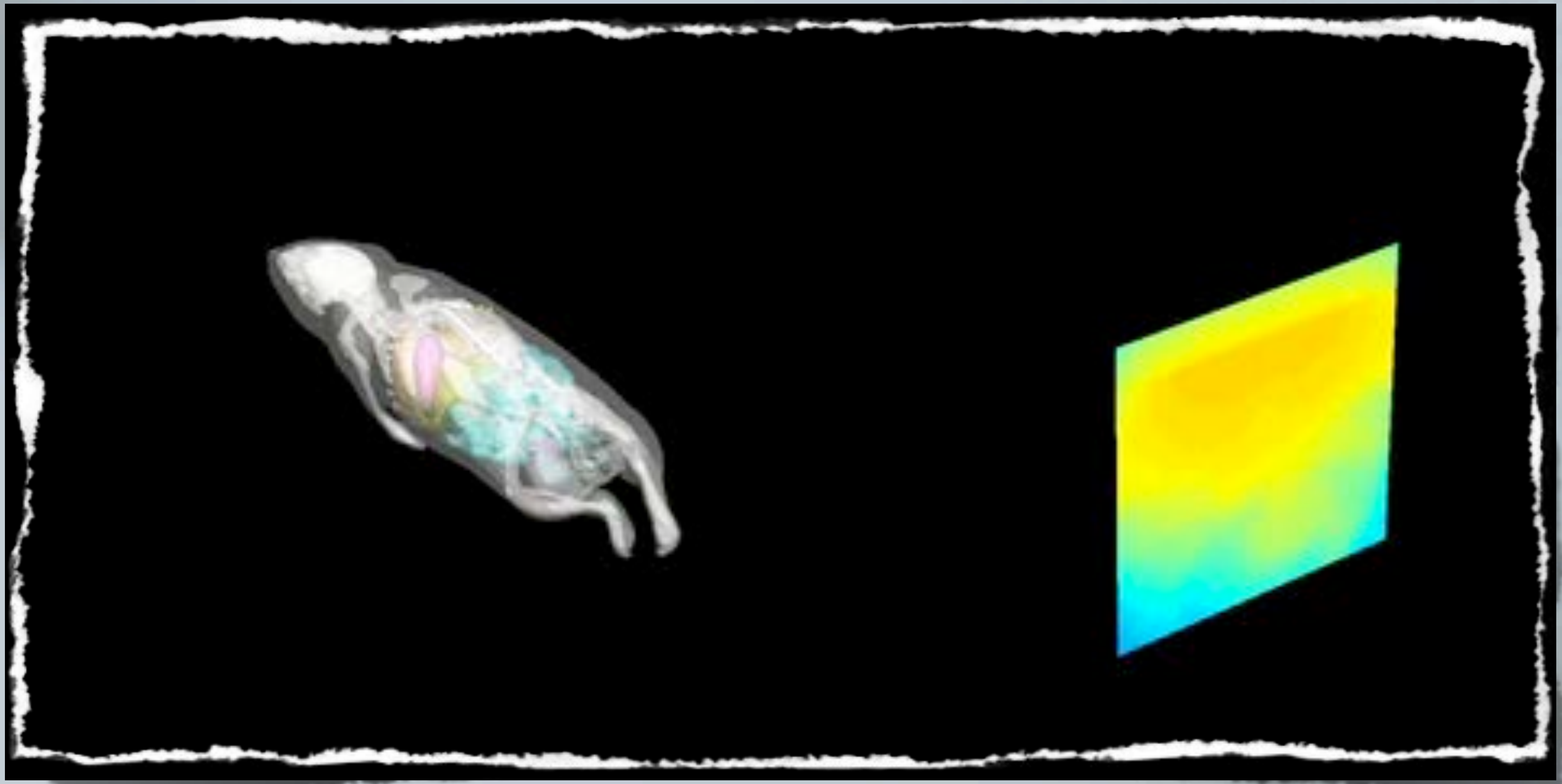

Outline

- The fluorescence phenomenon.
- Fluorescence molecular imaging – the problems.
- Image acquisition systems.
- Light propagation models.
- Conclusion.

Conclusion

Contribution of the research

- Solution of the forward problem in fluorescence molecular imaging with utilization of the RTE model.
- Solution of the forward problem in fluorescence molecular imaging with the dual coupled RTE-DA model.
- Development of an epi-illumination fluorescence molecular imaging with scanning structured excitation source.
- Fluorescence acquisition with angular information.

Conclusion

Ongoing research

- Development of an inverse problem solution, based on super-ellipsoidal models and the Levenberg-Marquardt technique.
- Further evaluation of the dual coupled RTE-DA model on non-homogeneous synthetic phantoms.
- Optimization of the algorithms for time efficacy increase.

Conclusion

Possible prospects

- Optimization of the spatial and angular discretization schemes.
- Investigation of the possibility to apply the RTE based forward solver.
- Study of the molecular information of the biomarkers.
- Development of small animal tomographic applications.
- Adaptation of the methodology for breast cancer detection.
- Development of a compact and portable system!

Conclusion

Is the solution of the reconstruction problem the border of this field?

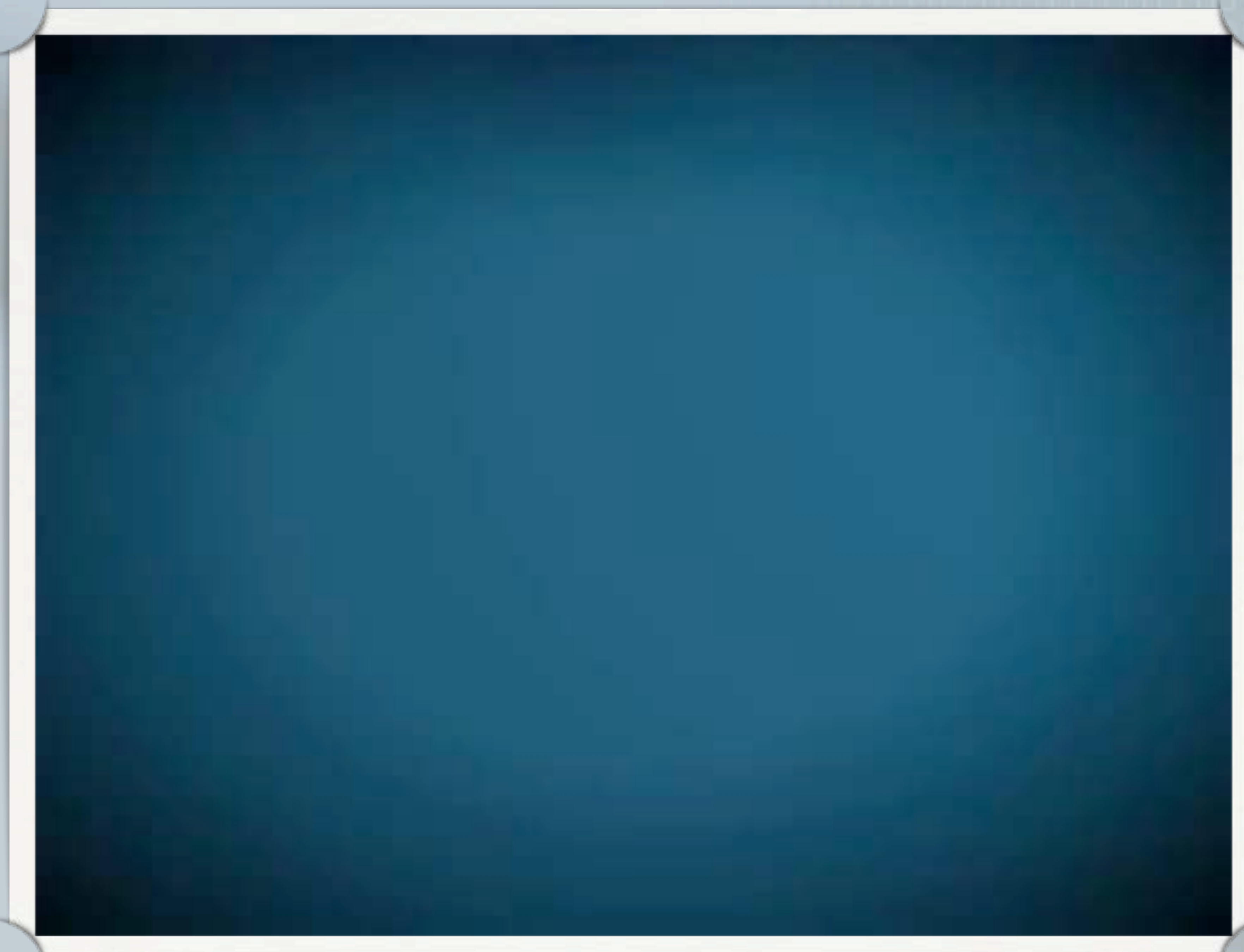

Thank you for your attention!!!

dgorpas@iti.gr